Behavioral/Cognitive

Memory Specific to Temporal Features of Sound Is Formed by Cue-Selective Enhancements in Temporal Coding Enabled by Inhibition of an Epigenetic Regulator

Elena K. Rotondo and Kasia M. Bieszczad
Department of Psychology, Rutgers, The State University of New Jersey, Piscataway, New Jersey 08854

Recent investigation of memory-related functions in the auditory system have capitalized on the use of memory-modulating molecules to probe the relationship between memory and substrates of memory in auditory system coding. For example, epigenetic mechanisms, which regulate gene expression necessary for memory consolidation, are powerful modulators of learning-induced neuroplasticity and long-term memory (LTM) formation. Inhibition of the epigenetic regulator histone deacetylase 3 (HDAC3) promotes LTM, which is highly specific for spectral features of sound. The present work demonstrates for the first time that HDAC3 inhibition also enables memory for temporal features of sound. Adult male rats trained in an amplitude modulation (AM) rate discrimination task and treated with a selective inhibitor of HDAC3 formed memory that was highly specific to the AM rate paired with reward. Sound-specific memory revealed behaviorally was associated with a signal-specific enhancement in temporal coding in the auditory system; stronger phase locking that was specific to the rewarded AM rate was revealed in both the surface-recorded frequency following response and auditory cortical multiunit activity in rats treated with the HDAC3 inhibitor. Furthermore, HDAC3 inhibition increased trial-to-trial cortical response consistency (relative to naive and trained vehicle-treated rats), which generalized across different AM rates. Stronger signal-specific phase locking correlated with individual behavioral differences in memory specificity for the AM signal. These findings support that epigenetic mechanisms regulate activity-dependent processes that enhance discriminability of sensory cues encoded into LTM in both spectral and temporal domains, which may be important for remembering spectrotemporal features of sounds, for example, as in human voices and speech.

Key words: **auditory cortex; epigenetic; frequency follow response; HDAC3; memory; phase locking**

Significance Statement

Epigenetic mechanisms have recently been implicated in memory and information processing. Here, we use a pharmacological inhibitor of HDAC3 in a sensory model of learning to reveal the ability of HDAC3 to enable precise memory for amplitude-modulated sound cues. In so doing, we uncover neural substrates for memory's specificity for temporal sound cues. Memory specificity was supported by auditory cortical changes in temporal coding, including greater response consistency and stronger phase locking. HDAC3 appears to regulate effects across domains that determine specific cue saliency for behavior. Thus, epigenetic players may gate how sensory information is stored in long-term memory and can be leveraged to reveal the neural substrates of sensory details stored in memory.

Received Mar. 31, 2021; revised July 23, 2021; accepted Aug. 18, 2021.

Author contributions: E.K.R. and K.M.B. designed research; E.K.R. performed research; E.K.R. analyzed data; E.K.R. and K.M.B. wrote the paper.

This work was supported by National Institutes of Health Grants R03-DC014753 (to K.M.B.) and R01-DC018561 (to K.M.B.), the American Speech-Language-Hearing Foundation 2017 New Century Scholars Grant (to K.M.B.), and the Brain and Behavior Research Foundation 2017 National Association for Research on Schizophrenia and Depression Young Investigator Award (to K.M.B.). We thank Justin Yao and Dan Sanes of the Center for Neural Science at New York University for sharing MATLAB code to analyze cortical representations of amplitude modulation rates.

The authors declare no competing financial interests.

Correspondence should be addressed to Elena K. Rotondo at elena.rotondo@rutgers.edu.

https://doi.org/10.1523/JNEUROSCI.0691-21.2021

Introduction

In humans and other species, precise representation of temporally modulated auditory signals is critical for identification and discrimination among communication sounds. Individual differences in response timing, response consistency, and magnitude of phase-locked activity of the sound-evoked neural responses are associated with auditory behavioral ability (Hornickel et al., 2009, 2012; Anderson et al., 2011, 2012, 2013; Centanni et al., 2014; Kraus et al., 2014; Strait et al., 2012; Tierney et al., 2015; von Trapp et al., 2016; Omote et al., 2017; Thompson et al., 2017; White-Schwoch et al., 2017; Otto-Meyer et al., 2018), and can be enhanced by learning (Beitel et al., 2003; Bao et al., 2004; Hornickel et al.,

2012; Kraus et al., 2014; Tierney et al., 2015; von Trapp et al., 2016). Indeed, experience can engender stimulus-specific neural enhancements for coding the temporal features of behaviorally relevant sounds (Bao et al., 2004; Song et al., 2008; Strait et al., 2012).

This study aimed to identify the auditory system substrates of newly formed memory that is specific to temporal features of sound. To do so, an epigenetic memory-modulating molecule—histone deacetylase 3 (HDAC3)—was leveraged to determine effects on temporal neural coding for temporal features of sound. It revealed novel relationships between individual differences in behavioral ability and neural substrates in the auditory system. Epigenetic mechanisms leave a physical impression from experience, which can lead to changes in cell function that give rise to long-lasting changes in behavior (Campbell and Wood, 2019). Histone acetylation is a key chromatin modification controlled by HDACs, which usually negatively regulate gene expression. Thus, HDAC deletion or inhibition facilitates transcription during memory consolidation and enhances lasting forms of synaptic plasticity (McQuown et al., 2011). The focus on HDAC3 is determined by its role as a class I HDAC (with primary function in the cell nucleus) to bidirectionally regulate activity-dependent acetylation, whose inhibition has been shown in various tasks and species to facilitate the formation of persistent memory (Stefanko et al., 2009; Malvaez et al., 2010; Gervain et al., 2013; Bieszczad et al., 2015; Phan et al., 2017; Hitchcock et al., 2019; Shang et al., 2019; Rotondo and Bieszczad, 2020, 2021). In auditory models of learning, HDAC3 inhibition (HDAC3i) facilitates highly specific memory for spectral features of sounds like acoustic frequency, with both cortical and subcortical sequelae (Bieszczad et al., 2015; Phan et al., 2017; Shang et al., 2019; Rotondo and Bieszczad, 2020, 2021). HDAC3 may epigenetically control systems-level informational capture for sensory information to determine the amount and type of information being consolidated into persistent memory (Phan and Bieszczad, 2016; Campbell and Wood, 2019). Here, rats were trained to discriminate temporal cues among amplitude modulation (AM) rates either with or without treatment with a pharmacological HDAC3-inhibitor (RGFP966). AM was imposed on a broadband noise carrier, which virtually eliminated spectral cues available to rats and encouraged learning about AM rate. Following training, auditory cortical and subcortical responses were evoked by AM stimuli to determine learning-induced auditory systemwide plasticity and integration changes in the representation of temporal sound cues, the relationship of these cues to memory specificity for temporal cues, and whether either were facilitated by HDAC3 inhibition. This is the first study to address the role of HDAC3 in temporal information encoding for auditory memory and learning-induced auditory system plasticity. Facilitating cortical and subcortical integration/coordination of experience-dependent enhancements for behaviorally significant features of sound might enable the encoding of persistent and vivid memories integral to hearing, speech, language, reading, and musical abilities. Here, HDAC3-inhibition is applied to reveal how its effects extend to temporal forms of auditory processing that promote the precise storage of sensory details into associative memory to enable discriminative learned behavior.

Materials and Methods

Subjects

A total of 21 adult male Sprague Dawley rats (275–300 × g on arrival; Charles River Laboratories) were used (RGFP966, $n = 8$; vehicle, $n = 8$; naive, $n = 5$) in behavioral and electrophysiological procedures. In sum, these rats represent the following separate groups: (1) treated vehicle, rats received vehicle injections during amplitude modulation rate discrimination training; (2) treated RGFP966, rats that received injections of the HDAC3 inhibitor RGFP966 during amplitude modulation rate discrimination training; and (3) naive, rats did not receive training in the auditory task and were used exclusively for baseline comparison of cortical electrophysiology. All animals were individually housed in a colony room with a 12 h light/dark cycle. Throughout behavioral procedures, rats were water restricted, with daily supplements provided to maintain them at ~85% free-drinking weight. All procedures were approved and conducted in accordance with guidelines by the Institutional Animal Care and Use Committee at Rutgers University.

Behavioral procedures and analysis

All behavioral sessions were conducted in instrumental conditioning chambers within a sound-attenuated box. All subjects initially learned how to press a lever for water reward in five sessions of ~45 min bar-press shaping before beginning the experimental timeline shown in Figure 1. This phase of training ensured that all animals could acquire the procedural aspects of the task (i.e., bar pressing for rewards) before any sounds were introduced.

Next, rats received tone–tone discrimination training. The purpose of training rats to discriminate tone frequency was to establish that animals could perform the procedural aspects of the task under discrimination conditions (i.e., go vs no go). Further, it offered a way of measuring individual tendencies to form general or specific memories in a sound dimension other than the temporal cues under study and without any treatment with drugs.

Rats learned to discriminate between a rewarded sound, called the S+, and an unrewarded sound, called the S−. Rats learned to respond to a 5 kHz pure tone S+ stimulus (8 s, 70 dB) for operant reward and to withhold responding from a 9.8 kHz pure tone S− stimulus (8 s, 70 dB). Responses to the S− or during the silent intertrial interval resulted in a visual error signal and triggered an 8 s time-out that extended the time until the next sound trial. Tone–tone discrimination training accomplished two goals. First, rats learned to bring operant behavior under control of sound cues (rather than silence). Second, rats learned the structure of a discrimination task. Tone–tone discrimination training continued until rats reached criteria performance for 2 consecutive days (or a maximum of 20 training sessions). Criteria were (1) >70% of all responses occurring in the presence of sound (vs silence), (2) ≥90% response rate to S+ trials, and (3) ≤25% response rate to S− trials.

Twenty-four hours following the final tone–tone discrimination training session, rats were given a tone memory test, during which 8 pure tone frequencies were presented 12 times each in a pseudorandom order: 3.1, 4.0, 5.0, 6.2, 8.0, 9.8, 12.3, and 16.0 kHz. No responses were reinforced. The purpose of this test was to increase experimental control by determining which animals may have been predisposed to signal-specific memory to increase experimental control before drug treatment manipulation.

To create performance-matched groups for the remainder of the experiment, measures of performance during tone–tone discrimination training and of memory specificity as revealed by the tone memory test were used to create performance-matched groups for the remainder of the experiment (see below, Behavioral statistical analysis).

Forty-eight hours following the tone memory test, rats began AM rate discrimination training. The structure of the AM rate discrimination task was identical to that of the tone–tone discrimination task, except that rats were required to discriminate the AM rate of broadband noise rather than acoustic frequency of pure tones. AM broadband noise (modulation depth, 100%; noise spectrum, 800–12 000 Hz; 8 s, 70 dB) was presented at two different amplitude modulation rates, 18.5 Hz (S+) and 155 Hz (S−). Each sound trial was separated by a variable intertrial interval (mean = 15 s; range = 5–25 s). Rats learned to respond to the S+ for a reward. Bar presses to the S− or the silent intertrial interval triggered a visual error signal and an 8 s time-out period. All rats were trained to performance criteria (or a maximum of 12 training sessions). Criteria were (1) >70% of all responses occurring in the presence of

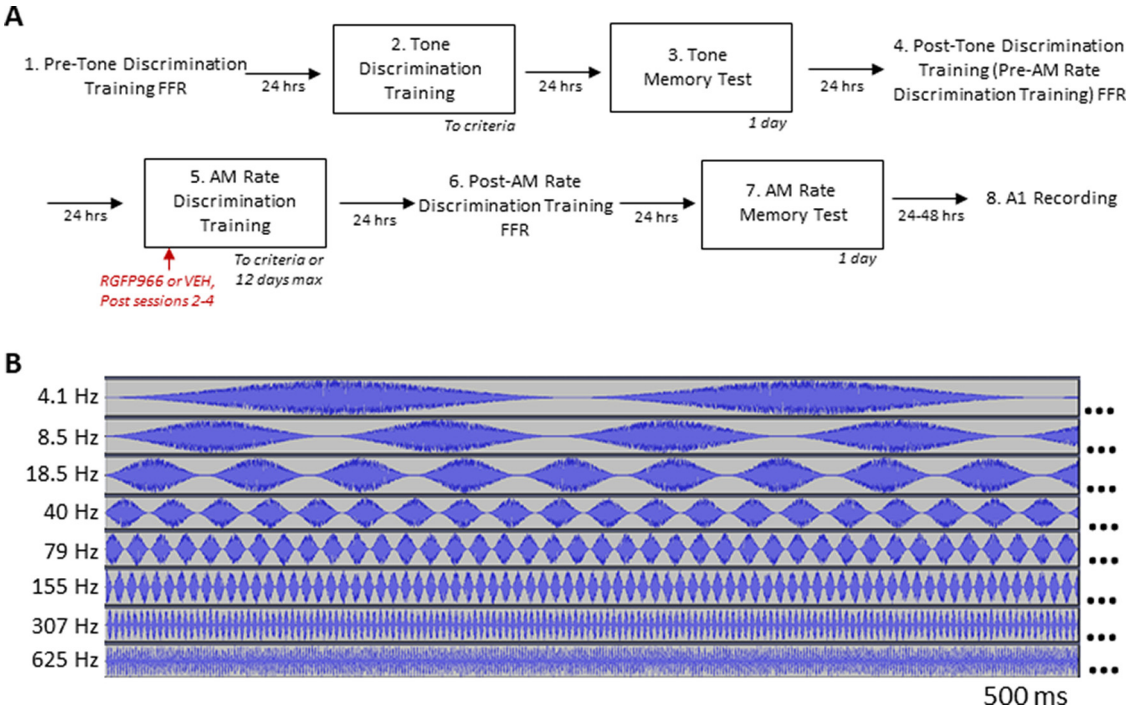

Figure 1. Experimental timeline. ***A***, Rats underwent the following four behavioral phases (indicated in boxes): tone discrimination training, followed by a tone memory test, followed by AM rate discrimination training, followed by an AM rate memory test. Twenty-four hours before tone discrimination training, AM rate discrimination training, and the AM rate memory test, an AM noise-evoked FFR was recorded. Twenty-four to 48 h after the AM rate memory test, tone- and AM-noise-evoked responses in the primary auditory cortex were recorded. ***B***, A 500 ms excerpt of sound stimulus waveforms is shown for each AM rate used for behavioral training and testing and electrophysiological recordings. Sounds were presented at different duration depending on experimental phase and AM rate, so the ellipses indicate that sound duration often extended beyond the 500 ms shown here. Note that all AM sounds had an 8 s duration when used in behavioral tasks, whereas AM sound duration was varied by rate to capture 5 or 10 modulation cycles for FFR and cortical recordings, respectively.

sound (vs silence), (2) ≥90% response rate to S+ trials, and (3) ≤25% respond rate to S− trials**.** AM rate discrimination training performance was calculated and statistically analyzed as described above for tone–tone discrimination training.

Forty-eight hours following the final AM rate discrimination training session, rats were tested in an AM rate memory test to reveal memory specificity for signal AM rates. During the memory test, eight AM rates were presented 12 times each in a pseudorandom order: 4.1, 8.5, 18.5, 40, 79, 155, 307, and 625 Hz. No responses were reinforced.

HDAC3 manipulation

HDAC3 is a transcriptional regulator that typically represses gene expression through chromatin modification (McQuown et al., 2011). The pharmacological HDAC3 inhibitor, RGFP966 (10 mg/kg), was used as previously described (Bieszczad et al., 2015) to facilitate learning-induced neural mechanisms of auditory memory formation. RGFP966 at this dose is known to remove HDAC3-mediated constraints on gene expression by physically decreasing the interaction between HDAC3 and relevant gene promoters and concurrently increasing local acetylation to allow an open state of chromatin that is permissive to gene expression (Malvaez et al., 2013). Rats were assigned to either the RGFP966 (n = 8) or vehicle (n = 8) before AM rate discrimination training so that groups were matched with respect to tone–tone discrimination performance and any predisposition to memory specificity as revealed by the tone memory test (see above, Behavioral procedures and analysis). Rats received 3 consecutive days of postsession, subcutaneous injections of RGFP966 (10 mg/kg) or vehicle (equated for volume; dose established, Malvaez et al., 2013, and confirmed in auditory system function, Bieszczad et al., 2015) immediately following each of three daily AM rate discrimination training sessions (2–4). Post-training pharmacological treatment confines manipulation to the memory consolidation period, which is classically defined as a <6 h window following the training event (McGaugh, 2000) while avoiding potential confounding effects based on perception or motivation during task performance or within-session learning. For the remainder of training sessions, all rats received postsession injections of saline (equated for volume) to ensure that any effect of the injection itself remained consistent throughout training until reaching performance asymptote.

Auditory cortical recording procedure and analysis

To determine changes in auditory cortical response to AM noise, electrophysiological recordings were obtained from anesthetized subjects (total n = 21 rats; sodium pentobarbital, 50 mg/kg, i.p.) in an acute, terminal recording session 24–48 h following the AM rate memory test. Recordings were obtained from trained animals (vehicle and RGFP966) and a group of experimentally naive animals that did not receive behavioral training or drug treatment. All recordings were made in a recording chamber completely separate from the training chamber and while the animal was anesthetized, which is a different state and context than that used in training. Therefore, any differences in responses measures from trained versus naive rats are interpreted to be robust and lasting changes to the auditory system's response to sound that is not context dependent nor dependent on short-term arousal or attention processes during active task engagement. All recordings were performed inside a double-walled, sound attenuated room using a linear array (2 × 3) of parylene-coated microelectrodes (1–2 MΩ, 250 µm apart) targeted to the middle cortical layers (III–IV, 400–600 µm orthogonal to the cortical surface) of the right primary auditory cortex (A1). Multiple penetrations (six contacts per penetration) were performed across the cortical surface, with an average of 27.04 (SE = 2.48) sites identified as within A1 per animal.

Acoustic stimuli were presented to the left ear from a speaker positioned ~10 cm from the ear. Two sets of sounds were used. The first set of sounds was 50 ms pure tones (1–9 ms cosine-gated rise/fall time) presented in a pseudorandom order (0.5–54.0 kHz in half-octave steps; 70 dB SPL; 10 repetitions) with a variable interstimulus interval average of 700 ± 100 ms. This set enabled a rough determination of frequency tuning. The second set was AM broadband noise (modulation depth, 100%; noise spectrum, 800−12,000 Hz) presented in pseudorandom

order (4.1, 8.5, 18.5, 40, 79, 155, 307, and 625 Hz modulation rates; and unmodulated noise; 70 dB SPL; 20 repetitions) with a variable interstimulus interval average of 1600 ± 300 ms. The duration of each stimulus was the time it takes to complete 10 full cycles of modulation (range, 16.0–2439.02 ms). The unmodulated noise had a duration of 580.71 ms, which represents the average duration of all AM stimuli, and was used to confirm that the recording sites were sound responsive.

Neural activity was amplified times 1000 and digitized for subsequent off-line spike detection and analysis using custom MATLAB scripts. Recordings were bandpass filtered (0.3–3.0 kHz). Multiunit discharges were characterized using previously reported temporal and amplitude criteria (Elias et al., 2015). Acceptable spikes were designated as waveforms with peaks separated by no more than 0.6 ms and with a threshold amplitude >1.5 (for the positive peak) and <2.0 (for the negative peak) × rms of 500 random traces from the same recording on the same microelectrode for each site. Responses greater than ±1.0 SEM of the spontaneous spike rate were considered true sound-evoked responses.

Frequency following response recordings

The surface-recorded frequency following response (FFR), which measures neural activity phase locked to sound, was recorded three times in anesthetized rats [ketamine-xylazine; ketamin: 90 mg/kg, xylazine: 11 mg/kg, i.p.) to determine learning-induced changes in subcortical processing of sound (1) 24 h before tone–tone discrimination training, (2) 24 h before AM rate discrimination training, and (3) 24 h following the final AM rate discrimination training session. All recordings were made in a recording chamber completely separate from the training chamber and while the animal was anesthetized, which is a different state and context than that used in training. Stimulus presentation and neural response recordings were conducted using BioSigRZ software (Tucker Davis Technologies). Evoked potentials were recorded using a three-electrode configuration, with subdermal needle electrodes (1 kΩ) positioned at the midline along the head (recording), immediately below the left pinna (reference), and the midline on the back of the neck (ground). Sound stimuli were 70 dB SPL, AM broadband noise presented to left ear from a speaker positioned 8 cm away. Four AM rates (18.5, 40, 79, and 155 Hz) were presented in a blocked format (1500 stimuli per block, each block repeated two times). Stimulus duration varied according to AM rate to complete five full modulation cycles (range 32.26–270.27 ms). The presentation rate ranged from 2.4 Hz to 10.1 Hz. Recordings were low-pass filtered online at 3 kHz and high-pass filtered online at 10 Hz, with a notch filter at 60 Hz.

Experimental design and statistical analysis

Group sizes are consistent with prior reports showing brain–behavior relationships in rodent models of auditory memory, including with the use of an HDAC3 inhibitor (Bieszczad and Weinberger, 2010; Rotondo and Bieszczad, 2020, 2021). Measures of the frequency following response are within subject, providing additional power to detect significant differences. Finally, correlative data between measures of neural plasticity and learned behavior further validate the current findings. All statistical analyses were performed using IBM SPSS software.

Behavioral statistical analysis

Sixteen adult male Sprague Dawley rats (RGFP966 $n = 8$; vehicle $n = 8$) were used in the behavioral experiment. To create performance-matched groups before AM rate discrimination training, measures of performance during tone–tone discrimination training and of memory specificity as revealed by the tone memory test were calculated and equated among groups. Metrics used to equate tone–tone discrimination training performance included (1) the number of training days to criteria, (2) response rate to S+ trials during the first two versus last two training sessions, (3) response rate to S− trials during the first two versus last two training sessions, (4) the difference in response rate to S+ versus S− trials during the first two versus last two training sessions, and (5) sound control (percentage of responses occurring to sound vs silence) during the first two versus last two training sessions. Metric 1 was analyzed with an independent samples t test, whereas metrics 2–5 were analyzed using a mixed-model ANOVA with the factors drug treatment condition and session.

Metrics used to equate tone memory specificity revealed by the tone memory test included the following: (1) percentage of responses to the S+ frequency minus percentage of response to the S− frequency, where positive values indicate greater responding to the S+ than S− frequency. (2) For the S+ frequency, two contrast measures were calculated as follows: percentage of responses to S+ frequency minus (average percentage of response to the nearby novel frequencies, 4.0 kHz and 6.2 kHz) and percentage of responses to S+ frequency minus (average percentage of responses to distant novel frequencies, 3.1 and 8.0 kHz). Positive values indicate greater responding to the S+ than novel frequencies. (3) For the S− frequency, two contrast measures were calculated as follows: percentage of responses to S− frequency minus (average percentage of response to the nearby novel frequencies, 8.0 and 12.3 kHz) and percentage of responses to S− frequency minus (average percentage of responses to distant novel frequencies, 6.2 and 16.0 kHz). Negative values indicate less responding to the S− than novel frequencies. Additional metrics to examine group performance during the tone memory test included (1) sound control (percentage of responses occurring to sound vs silence) and (2) total number of bar presses to sound. All metrics were analyzed using an independent samples t test between drug treatment groups.

Metrics used to analyze performance during AM rate discrimination training were identical to those described above for tone–tone discrimination training. To quantify memory specificity for the signal AM rates, contrast measures of relative responses to AM rate were determined in three ways, analogous to those used for the tone memory test. (1) The difference in the percent of responses to the S+ and the S− was calculated, where positive values indicated greater responding to the S+ than the S− AM rate. (2) For the S+ AM rate, two contrast measures were calculated as follows: percentage of responses to signal AM rate minus (average percentage of response to the nearby AM rates, 8.5 Hz and 40 Hz) and percentage of responses to signal AM rate minus (average percentage of responses to distant AM rates, 4.1 and 79 Hz). Positive values indicate greater responding to the S+ AM rate than novel AM rates. (3) For the S− AM rate, two contrast measures were calculated as follows: percentage of responses to signal AM rate minus (average percentage of response to the nearby AM rates, 79 and 307 Hz) and percentage of responses to signal AM rate minus (average percentage of responses to distant AM rates, 40 and 625 Hz). Negative values indicate less responding to the S− AM rate than novel AM rates. All metrics were analyzed using an independent samples t test between drug treatment groups. In addition, a binomial test was used to test whether treatment with an HDAC3 inhibitor shifted the proportion of animals that fell into the top versus bottom half of memory specificity indices during the AM rate memory test compared with the tone memory test.

Auditory cortical recordings statistical analysis

Auditory cortical responses were compared among three groups: RGFP966-treated ($n = 8$), vehicle-treated ($n = 8$), and behaviorally naive ($n = 8$) rats. For group analyses, individual recording sites were treated as individual observations (see Table 5-Table 8 for sample sizes for each analysis. For each recording site, tone-evoked spike rate (spikes/s) were calculated by subtracting spontaneous spiking (40 ms window before tone onset) from evoked spiking within a 40 ms response-onset window (6–46 ms after each tone onset). Tone-evoked neural activity was used to determine tonotopy to identify recording sites within the A1. Best frequency (BF), the frequency to which the site responds to best at a given sound level (i.e., 70 dB) of each recording site was determined using evoked spike rate as a function of frequency. Sites that exhibit the characteristic progression from low to high BF along the posterior–anterior axis were classified as A1 and used for subsequent analyses. A chi-square test was used to test for group differences in the distribution of recording site BFs between groups.

Among recording sites within A1, AM noise-evoked multiunit activity was used to identify learning-induced changes in AM encoding by analyzing several measures. Figure 2 shows representative examples of

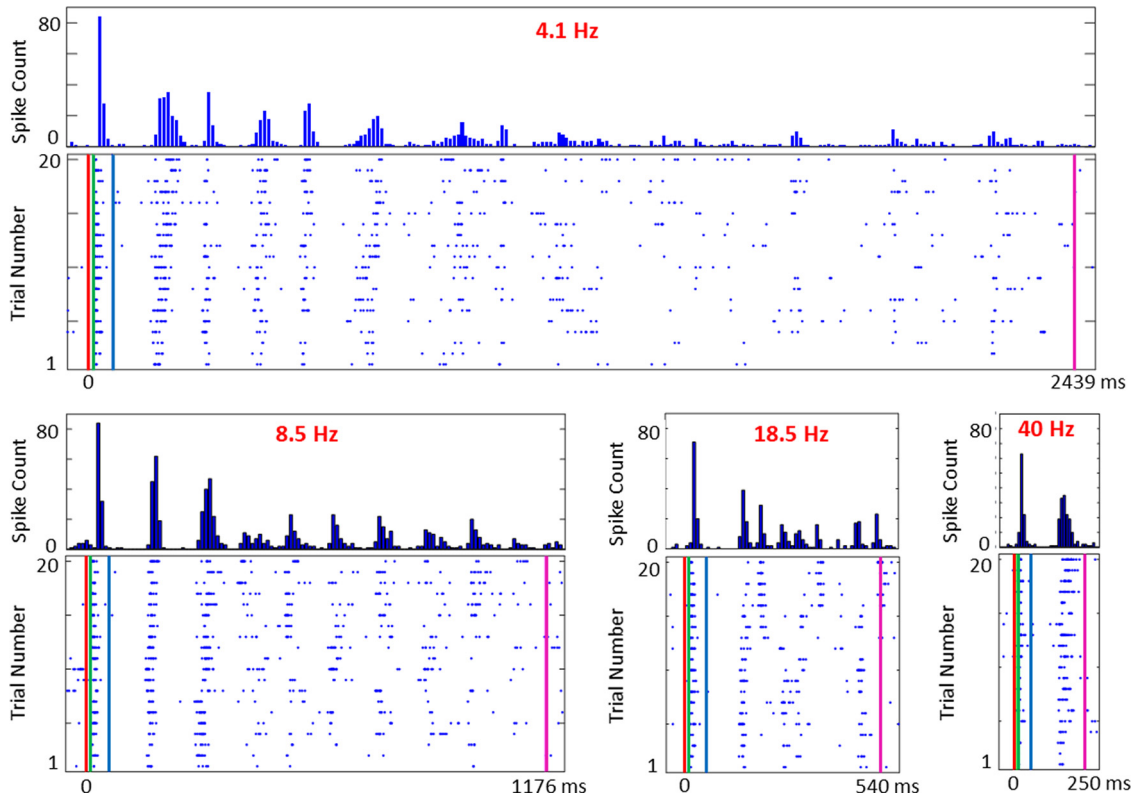

Figure 2. AM-noise-evoked auditory cortical responses. Eight different AM rates, ranging from 4.1 to 625 Hz, were used to evoke auditory cortical responses for analysis. Sound-evoked responses to four of these AM rates ranging from slow (4.1 Hz) to fast (40 Hz) are shown for illustrative purposes. Each AM rate was presented 20 times in a pseudorandom order, with responses to each trial represented in the spike rasters and collapsed across all trials for a given AM rate in the peristimulus time histogram. Each panel shows a 50 ms prestimulus period (to the left of the red line at the beginning of the trace) and a 50 ms poststimulus period (to the right of the magenta line near the end of the trace). The AM stimulus presentation began at 0 ms (on the *x*-axis) and ended at the magenta line labeled with a distinct duration that varied for each stimulus, which was played for 10 full AM cycles (e.g., the 4.1 Hz AM sound was 2439 ms in duration, and the 40 Hz AM sound was 250 ms in duration). For response consistency analysis, neural responses were analyzed from 12 ms after sound onset (indicated by the green vertical line in the raster plot) to sound offset (magenta line). For phase-locking analysis of AM rates $\leq$18.5 Hz, neural responses were analyzed from 60 ms after sound onset (indicated by the blue vertical line in the raster plot) to sound offset (magenta line).

sound-evoked cortical responses to AM sounds and indicates the time windows used for analyses as described below.

Phase locking. Vector strength (VS) and the Rayleigh statistic (RS) were calculated to determine how well evoked activity was time locked to the AM rates (Bao et al., 2004; Yao and Sanes, 2018, 2021) For each AM rate, evoked neural responses from a given recording site were analyzed from 60 ms after sound onset (to exclude onset responses) to the time of sound offset (to exclude any after-offset oscillatory responses) across 20 stimulus repetitions. Durations were set to the time needed to complete 10 AM cycles. Note that each sound was of a different duration to account for the different AM rates. VS was calculated across the evoked window as in previous studies (Goldberg and Brown, 1969; Bao et al., 2004; Yao and Sanes, 2018) as follows:

$$\text{vector strength (VS)} = (1/n)\sqrt{\Sigma(\cos(2\pi t_i(T))^2 + \Sigma(\sin(2\pi t_i(T))^2)}.$$

Here, t_i (i = 1, 2...n) is the time between the onset of the stimulus and the ith spike, where n is the total number of spikes, and T is th period of the amplitude modulation. One-way ANOVAs, followed by Holm–Bonferroni-corrected t tests, were used to determine group differences in vector strength in evoked responses.

The Rayleigh statistic, which estimates the significance of phase locking while controlling for the total number of spikes, was calculated as in previous studies (Mardia, 1972; Bao et al., 2004; Yao and Sanes, 2018) as follows:

Rayleigh statistic (RS) = (2) * (number of spikes) * (vector strength)^2.

The critical values for the Rayleigh statistic are 5.991, corresponding to $p < 0.05$, and 13.816, corresponding to $p < 0.001$. The threshold value of 5.991 was used to categorize sites into phase-locking or non-phase-locking responses to determine the proportion of recording sites that exhibited significant phase locking by subjects and by treatment group. A binomial test was used to test for significant differences in the proportion of phase-locked sites recorded from vehicle-treated or drug-treated rats, each independently compared with a group of untrained naive rats. In a subset of analyses of vector strength, only responses from phase-locked sites, as determined by the Rayleigh statistic, were used.

Response consistency. To determine within-stimulus response consistency in the AM-evoked neural responses, we used a k-means clustering approach over 20 individual trials of a given AM rate for each recording site. This approach generated a multidimensional hyperplane that represented spike counts across 5 ms time bins from 12 ms after sound onset (to account for neural transmission delays) to 12 ms after sound offset for each individual stimulus trial over 20 repetitions. The average spike count in time bins across trials was used to generate the centroid in the k-means cluster. The sum of distances from each repetition in the cluster to the centroid [sum of point-centroid distances (SUMD) in the kmeans MATLAB function] was used to represent the consistency of the AM-evoked cortical response to any unique stimulus. Lower SUMD values indicate greater response consistency (and lower response variability). One-way ANOVAs, followed by Holm–Bonferroni-corrected t tests, were used to determine group differences. Corrected p values are reported. Additionally, to test that the uneven number of individual data points (i.e., number of recording sites) among groups did not unduly influence our results, we performed a bootstrapping analysis in which an equal number subsample of the datasets are compared over 10,000 iterations. In each iteration, 40 recording sites were randomly sampled without replacement, and the average difference was calculated between

Table 1. Tone discrimination training performance metrics for subsequent drug treatment groups

		Sound control	S+ response rate (%)	S− response rate (%)	Δ S+ to S− response rate (%)
First two sessions	VEH ($n = 8$)	15.25 ± 1.72	26.03 ± 6.21	28.78 ± 7.18	−2.68 ± 1.98
	RGFP966 ($n = 8$)	14. 25 ± 1.69	24.64 ± 3.65	26.02 ± 3.21	−2.13 ± 2.83
Last two sessions	VEH ($n = 8$)	90.77 ± 1.09	98.56 ± 0.33	18.01 ± 1.40	80.47 ± 1.29
	RGFP966 ($n = 8$)	88.99 ± 1.80	97.88 ± 0.53	15.16 ± 1.34	83.84 ± 1.81

This table displays performance metrics for vehicle (VEH)- and RGFP966-treated rats during the first two versus last two training sessions, including sound control (% of total responses that occurred to sound as opposed to silence), S+ and S− response rate (percentage of S+ or S− trials with at least one response), and the difference between S+ and S− response rates. Data are displayed as mean ± SE.

naive versus vehicle-treated, naive versus RGFP966-treated, or vehicle-treated versus RGFP966-treated rats. After all iterations, a 98.75% confidence interval was calculated from the distribution, with a significant difference ($p < 0.05$) determined if at least 98.75% of the distribution of differences did not include zero. Finally, Pearson correlations were used to test for correlative relationships between cortical response consistency and phase locking. Finally, Pearson correlations were used to test for correlative relationships between cortical response consistency and phase locking.

Frequency following response recordings statistical analysis

FFRs were recorded at three time points for each of the 16 RGFP966- and vehicle-treated rats in the behavioral experiment (see Frequency following response recordings, above). Valid responses evoked by 79 Hz and 40 Hz AM rates were unable to be obtained for two subjects ($n = 1$ vehicle treated; $n = 1$ RGFP966-treated; see Table 9 for sample sizes used in all FFR analyses).

Three analyses were used to determine changes in the FFR. In each case, values were compared pre- to post-training in each individual subject to measure learning-induced changes.

Response magnitude (dB). To determine response magnitude of phase-locked neural activity evoked by a given AM rate, a fast Fourier transform (FFT) was applied to the filtered averaged waveform (representing the average of both 1500 stimulus blocks, i.e., response to 3000 stimulus repetitions). Before performing the FFT, a Hanning window was applied to the signal to minimize the effects of direct current offset on the resulting spectrum. Response magnitude (dB) of each response was calculated as follows:

$$\text{Response magnitude (dB)} = 10\log \frac{\text{spectral magnitude of evoked FFRs at frequency of AM rate } (\mu\text{V})}{\text{spectral magnitude of silent period FFRs at frequency of AM rate } (\mu\text{V})}.$$

The difference in response magnitude as a function of learning was determined by subtracting pretraining response magnitude from post-training response magnitude for each individual rat.

Response consistency (Fisher z). Response consistency is a measure that captures variation in both timing and morphology of cue-evoked responses. The average responses to each 1500-trial block of a given stimulus were used to derive measures of response consistency in the FFR. This method of analyzing response consistency has been previously validated, and published comparisons have shown a high correlation ($r = 0.98$) among the first block versus last block of trials and bootstrapping techniques based on single-trial FFR data (Hornickel and Kraus, 2013; Krizman and Kraus, 2019). The two subaverages were correlated to produce an r value, where higher r values indicate better response consistency. Because the r value distribution is not normal, a Fisher z transformation was applied to the r values to increase the spread of the data. The difference in transformed r values at the pre- versus post-training time point was calculated for each individual and for each AM rate.

Timing jitter (ms). Like response consistency, timing jitter measures trial-to-trial variability in the neural response. However, timing jitter captures variability in the timing of the response independently from cue-evoked response morphology (by excluding, e.g., response amplitude). The average responses to each 1500-trial block of a given stimulus were used to derive measures of jitter in the FFR. The two subaverages were cross-correlated, that is, shifted in time relative to each other, to determine the timing lag that produces the highest r value. The difference in the absolute value of the timing lag was calculated at the pre- versus post-training time point for each individual and for each AM rate. Negative difference values indicate less timing jitter as a function of training so that the timing of the response is more consistent across subaverages.

FFR data were analyzed using a series of Holm–Bonferroni-corrected t tests. Single-sample t tests were used to determine whether a particular aspect of the FFR (response magnitude, consistency, or jitter) was significantly altered over the course of learning. Independent samples t tests were used to determine whether the change in a particular aspect of the FFR was different among the drug treatment groups.

One caveat in the present design is that the FFR likely reflects activity of both cortical and subcortical sources for the slower S+ AM rate (18.5 Hz), whereas responses evoked by the faster AM rates will predominantly be of subcortical origin (Joris et al., 2004; Anderson et al., 2006; Fitzpatrick et al., 2009; Coffey et al., 2016). Therefore, all neural responses evoked by the S+ in this study will include a cortical component, precluding the ability to localize plasticity to only subcortical (vs cortical) levels of the auditory system. Nonetheless, the design does provide the opportunity to validate our prior cortical findings using multiple recording methods and neural generators. On the other hand, the design does enable the observation of coordinated and integrated plasticity across cortical and subcortical levels for the faster S− AM rate (155 Hz).

Brain–behavior correlative data

To limit the number of statistical comparisons, we set the a priori criterion that brain–behavior Pearson correlations would be pursued only for brain measures that showed signal-specific, learning-induced plasticity. The number of subjects available for each correlation (determined by subject attrition in neural measures; see above, Auditory cortical recordings statistical analysis and Frequency following response recordings statistical analysis) is detailed in Table 10.

Measures used for Pearson correlations are as follows. For behavioral measures, the percentage of responses to the 18.5 Hz S+ was used as an index of memory specificity as it was strongly correlated with other indices of memory specificity (% bar presses to S+ vs Δ % bar presses to S+ vs S−, $r = 0.981$, $p < 0.00{,}001$; vs Δ % bar presses to S+ vs nearby neighbors, $r = 0.987$, $p < 0.00{,}001$; vs Δ % bar presses to S+ vs distant neighbors, $r = 0.976$, $p < 0.00{,}001$). For FFR data, the change in response magnitude over the course of AM rate discrimination training in FFRs evoked by the 18.5 Hz was used for each subject. For auditory cortical data, an average value was computed for each subject for vector strength, the Rayleigh statistic, and percentage of phase-locked sites.

Results

Groups perform identically during tone discrimination training and memory testing, before administration of the HDAC3 inhibitor

All rats were first trained in a tone discrimination task to bring operant responding under the control of sound and teach rats the procedural aspects of a discrimination task. Subsequently, rats underwent a tone memory test to determine the specificity with which they remembered the rewarded S+ (5.0 kHz) and unrewarded S− (9.8 kHz) tones. Behavioral performance during both training and testing was used to create behaviorally

Table 2. Performance during the Tone Memory Test

	Δ % Bar presses to S+ vs. S−	Δ % Bar presses to S+ versus nearby tones	Δ % Bar presses to S+ versus distant tones	Δ % Bar presses to S− versus nearby tones	Δ % Bar presses to S− versus distant tones
VEH ($n = 8$)	33.24 ± 4.17	17.79 ± 5.13	25.17 ± 5.16	−3.94 ± 1.85	−5.26 ± 1.85
RGFP966 ($n = 8$)	28.80 ± 6.26	14.10 ± 7.07	20.50 ± 5.55	−0.13 ± 1.42	−0.22 ± 0.82

This table displays relative measures of responding to tone frequencies presented during the tone memory test for subsequent vehicle (VEH)- and RGFP966-treated rats. On average, both groups responded more to the S+ than the S− and the neighboring novel tones. Both groups also responded less to the S− than the neighboring novel tones. Data are displayed as mean ± SE.

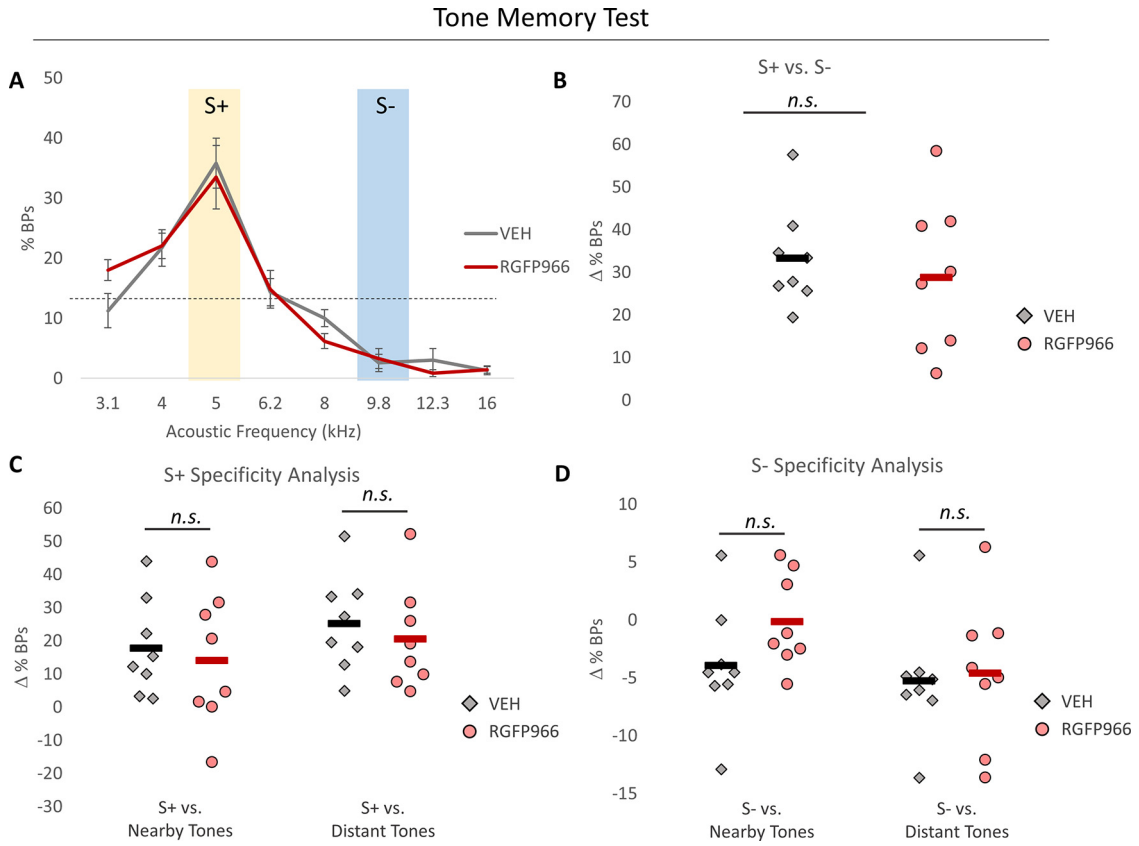

Figure 3. Before drug treatment, groups were matched for frequency specificity of memory in the tone memory test. Before the tone memory test, groups performed equally during tone–tone discrimination training. Rats showed significant improvement on each performance metric between the first two and last two training sessions (sound control: $F_{(1,14)} = 3030.713$, $p < 0.001$; S+ response rate: $F_{(1,14)} = 379.286$, $p < 0.001$; S− response rate: $F_{(1,14)} = 6.688$, $p = 0.022$; differences in S+ vs S− response rate: $F_{(1,14)} = 1420.594$, $p < 0.001$). No metric showed a significant main effect for drug condition (sound control: $F_{(1,14)} = 0.590$, $p = 0.455$; S+ response rate: $F_{(1,14)} = 0.088$, $p = 0.771$; S− response rate: $F_{(1,14)} = 0.608$, $p = 0.448$; difference in S+ vs S− response rate: $F_{(1,14)} = 1.117$, $p = 0.308$), and no metric showed a significant training session × drug condition interaction (sound control: $F_{(1,14)} = 0.081$, $p = 0.780$; S+ response rate: $F_{(1,14)} = 0.009$, $p = 0.925$; S− response rate: $F_{(1,14)} < 0.000$, $p = 0.987$; difference in S+ vs S− response rate: $F_{(1,14)} = 0.396$, $p = 0.539$; Table 1). ***A***, Groups exhibit similar response distributions across frequencies during the tone memory test. The dashed line represents the memory test gradient if responses were equally distributed among the frequencies, which would indicate a completely generalized memory. A score of zero would indicate no responses to a given test frequency, whereas a maximum score of 100 would indicate that all responses occurred to the indicated sound. The shape of the response distribution was quantified using relative measures of responding to S+, S−, and novel tone frequencies [Δ, percentage of bar presses (BPs)]. Data are presented as mean ± SE. ***B***, ***C***, Comparing these measures with independent samples *t* tests revealed no group differences in discrimination of the S+ frequency relative to (***B***) the S− or (***C***) the nearby and distant novel tone neighbors. ***D***, Independent samples *t* tests revealed no group differences in discrimination of the S− tone frequency from its nearby and distant novel tone neighbors. Dots represent individual subjects. Bars represent the group mean (Table 2).

equivalent groups before administration of the HDAC3 inhibitor in the following behavioral training phase (Tables 1, 2; Fig. 3).

Based on the subsequently assigned drug treatment conditions, the number of training days to reach criteria was equivalent among rats in the subsequently RGFP966-treated group (mean = 12.87, SE = 1.31) and the subsequently vehicle-treated group (mean = 11.75, SE = 1.26; $t_{(14)} = -0.616$, $p = 0.547$). Overall, rats showed significant improvement on each performance metric between the first two and last two training sessions. However, no metric showed a significant main effect for drug condition, and no metric showed a significant training session × drug condition interaction (Fig. 3). Group means and SEs are shown in Table 1.

Based on the subsequently assigned drug treatment conditions, independent samples *t* tests revealed that tone memory specificity was identical among groups after tone–tone discrimination training (Fig. 3; Table 2). Both groups made equal percentages of responses to the S+ and the S− and discriminated equally between the trained tone frequencies and novel tone frequencies. Here, it is important to note that under these conditions, both groups exhibited some degree of memory specificity insofar as the response distribution peaks at the S+ with minima near the S− (vs a generalized, flat response gradient) as would be predicted after discrimination training. In addition, to control for the magnitude of specificity effects, we ranked each rat from

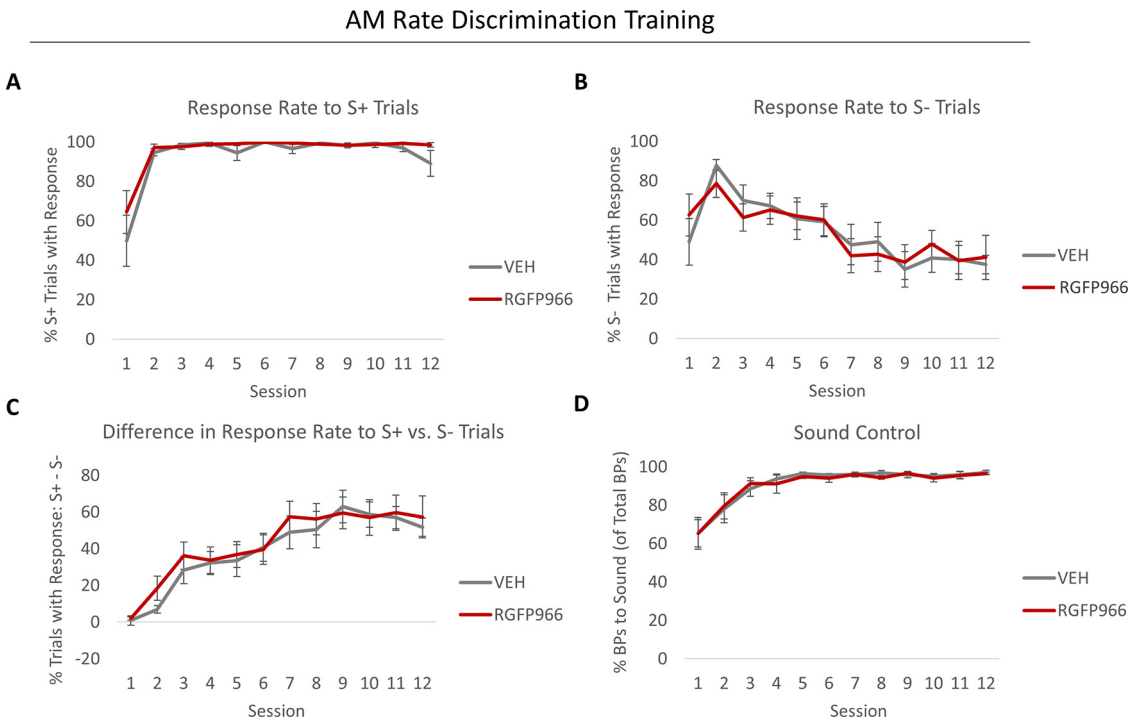

Figure 4. HDAC3 inhibition does not alter performance in the amplitude modulate rate discrimination task. ***A–D***, Performance metrics are equivalent between groups treated with RGFP966 and vehicle (VEH), including (***A***) response rate to S+ trials, (***B***) response rate to S− trials, (***C***) difference in response rate to S+ versus S− trials, and (***D***) sound control [percentage of bar press responses (BPs) occurring to either sound vs silence]. Overall, rats showed improved performance on all metrics between the first two and final two training sessions (sound control: $F_{(1,14)} = 24.263$, $p < 0.001$; S+ response rate: $F_{(1,14)} = 15.056$, $p = 0.002$; S− response rate: $F_{(1,14)} = 13.860$, $p = 0.002$; difference in S+ vs S− response rate: $F_{(1,14)} = 77.937$, $p < 0.001$). However, there was no main effect of drug treatment condition on any metric (sound control: $F_{(1,14)} = 0.001$, $p = 0.979$; S+ response rate: $F_{(1,14)} = 2.129$, $p = 0.167$; S− response rate: $F_{(1,14)} = 0.236$, $p = 0.634$; difference in S+ vs S− response rate: $F_{(1,14)} = 0.701$, $p = 0.417$), nor a significant drug treatment condition × session interaction (sound control: $F_{(1,14)} = 0.032$, $p = 0.860$; S+ response rate: $F_{(1,14)} = 0.141$, $p = 0.713$; S− response rate: $F_{(1,14)} < 0.001$, $p = 0.997$; difference in S+ vs S− response rate: $F_{(1,14)} = 0.099$, $p = 0.757$). Data is presented as mean ± SE.

greatest to smallest percentage of responses to the S+. This ranking revealed that four of the eight rats (i.e., 50%) were in the top half from each drug condition. Similarly, ranking each rat from greatest to smallest difference in the percentage of responses to the S+ versus S− revealed that four of the eight rats (50%) were from each drug condition. Other metrics reflecting aspects of performance other than specificity were also equivalent between groups during the tone memory test, including sound control [to-be RGFP966: mean = 83.48, SE = 3.14; to-be vehicle (VEH): mean = 88.93, SE = 1.84; $t_{(14)} = 1.465$, $p = 0.164$] and the number of bar presses to any sound (to-be RGFP966: mean = 37.25, SE = 5.55; to-be VEH: mean = 37.12, SE = 3.79; $t_{(14)} = -0.018$, $p = 0.985$). Together, these behavioral results show that there was no a priori difference between animals later assigned to vehicle- or RGFP966-treatment groups in relevant measures of sound-evoked bar-press responding or in tendency to remember sound specifically (to the S+ sound frequency) or generally across a spectral feature of sound, acoustic frequency. Therefore, subsequent differences in performance during AM rate discrimination training or the AM rate memory test can be attributed to the effects of HDAC3 inhibition, rather than procedural learning aspects of the task.

HDAC3 inhibition promotes memory specificity for AM rate

During AM rate discrimination training, rats received injections of either the HDAC3 inhibitor RGFP966 or vehicle immediately following each of three daily sessions 2–4. RGFP966- and vehicle-treated rats did not differ in the number of days of AM rate discrimination training before the AM rate memory test (RGFP966: mean = 11.62, SE = 0.37; VEH: mean = 11.62, SE = 0.37; $t_{(14)} = 0$, $p > 0.999$). Overall, rats showed improved performance on all metrics between the first two and final two training sessions. However, there was no main effect of drug treatment condition on any metric, nor a significant drug treatment condition × session interaction (Fig. 4; Table 3). Importantly, because groups did not differ in performance during AM rate discrimination training means that any subsequent behavioral differences during the AM rate memory test can be attributed to the remembered discriminability of AM stimuli alone.

The AM rate memory test revealed that RGFP966-treated rats formed memory for the rewarded S+ AM rate with greater specificity than vehicle-treated rats (Fig. 5; Table 4). Although all animals exhibited some degree of specificity with response distributions peaking at the S+ (as before after learning the tone–tone discrimination), HDAC3 inhibition produced a highly specific form of memory that resulted in greater behavioral discrimination between the S+ and the other test sounds than in vehicle-treated rats (Fig. 5; Table 4). To complement this analysis and control for the magnitude of effects, we again ranked each rat based on the percentage of responses to the S+. Seven of eight rats in the top half were treated with RGF966 (vs four of eight during the tone memory test; binomial test, $p = 0.038$). Similarly, seven of eight rats with the greatest difference in responding to the S+ versus S− were treated with RGFP966 (vs four of eight during the tone memory test; binomial test, $p = 0.038$). Therefore, treatment with RGFP966 increases the likelihood from a 50/50 chance

Table 3. AM rate discrimination training performance metrics for drug treatment groups

		Sound control	S+ response rate (%)	S− response rate (%)	Δ S+ versus S− response rate (%)
First two sessions	VEH ($n = 8$)	71.73 ± 6.84	72.29 ± 6.97	68.45 ± 5.82	3.84 ± 2.25
	RGFP966 ($n = 8$)	61.27 ± 10.57	80.79 ± 5.43	70.66 ± 7.07	10.12 ± 3.43
Last two sessions	VEH ($n = 8$)	96.41 ± 1.19	93.74 ± 3.57	36.04 ± 5.31	57.69 ± 5.53
	RGFP966 ($n = 8$)	91.04 ± 4.59	98.44 ± 0.86	38.18 ± 8.93	60.26 ± 8.90

This table displays performance metrics for vehicle (VEH)- and RGFP966-treated rats during the first two versus last two training sessions, including sound control (% of total responses that occurred to sound as opposed to silence), S+ and S− response rate (percentage of S+ or S− trials with at least one response), and the difference between S+ and S− response rate. Data are displayed as mean ± SE.

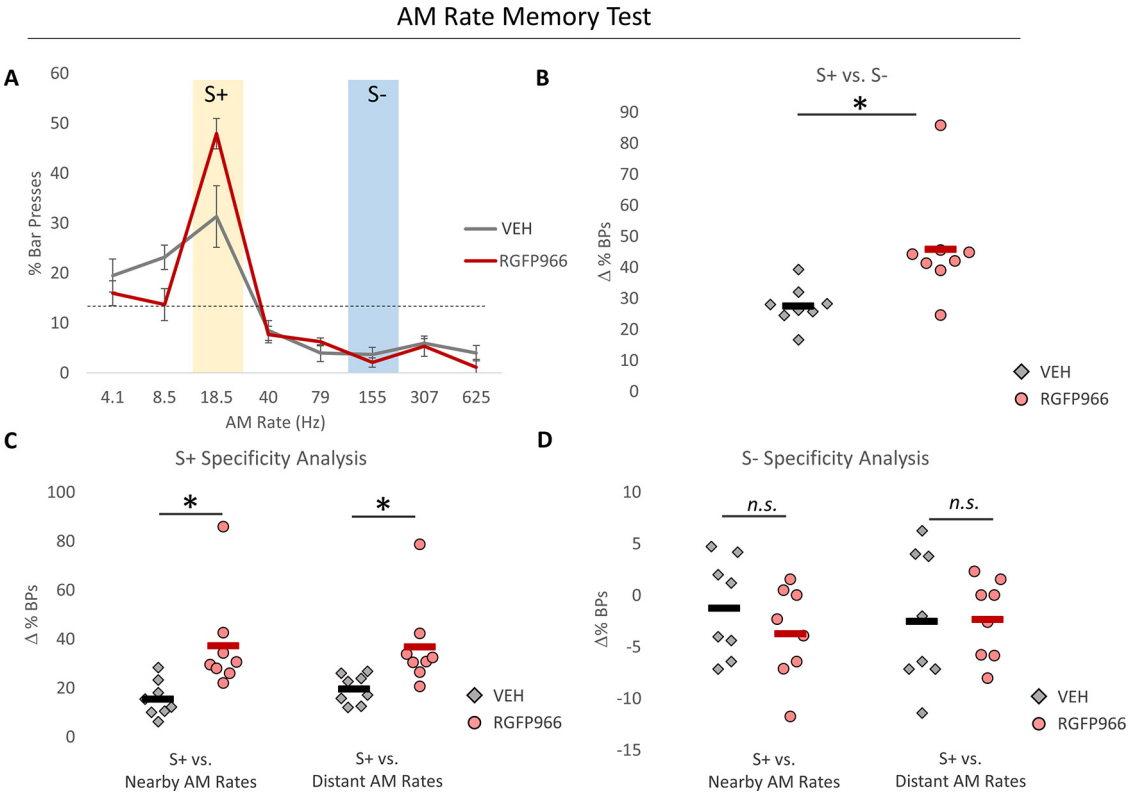

Figure 5. HDAC3 inhibition promotes memory specificity for AM rate. ***A***, RGFP966-treated rats exhibit an AM-rate-specific response distribution with a sharper peak at the S+ AM rate compared with vehicle (VEH)-treated rats. The dashed line represents the memory test gradient if responses were equally distributed among all AM rates, which would indicate a completely generalized memory. A score of 0 would indicate no responses to a given test frequency, and a maximum score of 100 would indicate that all responses occurred to the indicated sound. The shape of the response distribution was quantified using relative measures of responding to S+, S−, and novel AM rates [Δ, percentage of bar presses (BPs)]. Data are presented as mean ± SE. ***B***, ***C***, Independent samples *t* tests revealed that HDAC3-inhibited rats showed greater discrimination for the S+ AM rate from (***B***) the S− and (***C***) the nearby and distant novel AM rate neighbors compared with vehicle-treated rats. ***D***, Independent samples *t* tests revealed no group differences in discrimination of the S− AM rate from its nearby and distant novel AM rate neighbors. Dots represent individual subjects. Bars represents the group mean (Table 4).

Table 4. Performance during the AM Rate Memory Test

	Δ % Bar presses to S+ versus S−	Δ % Bar presses to S+ versus nearby AM rates	Δ % Bar presses to S+ versus distant AM rates	Δ % Bar presses to S− versus nearby AM rates	Δ % Bar presses to S− versus distant AM rates
VEH ($n = 8$)	27.59 ± 2.27	15.48 ± 2.60	19.58 ± 2.10	−1.23 ± 1.69	−2.51 ± 2.29
RGFP966 ($n = 8$)	**45.82 ± 6.17*[a]**	**37.23 ± 7.25*[b]**	**36.81 ± 6.34*[c]**	−3.70 ± 1.60	−2.32 ± 1.36

This table displays relative measures of responding to AM rates presented during the AM rate memory test for vehicle- and RGFP966-treated rats. On average, both groups responded more to the S+ than the S− and the neighboring novel tones. However, RGFP966-treated rats showed a greater response bias toward the S+ than vehicle-treated rats. Both groups also responded less to the S− than the neighboring novel tones, with no drug treatment group differences. Data are displayed as mean ± SE. Significant differences are bolded. *$p < 0.05$.

[a] $t_{(14)} = -2.277$, $p = 0.014$.
[b] $t_{(14)} = -2.819$, $p = 0.013$.
[c] $t_{(14)} = -2.576$, $p = 0.021$.

that an individual will develop greater memory specificity to the S+ relative to the group at large. In contrast, groups did not differ with respect to memory specificity for the unrewarded S− AM rate; responses to the S− stimulus during the memory test were equivalent (Table 4). Although the lack of effect on responses to the S− was surprising, given the prediction that HDAC3 inhibition will enhance memory specificity for all behaviorally relevant cues, this null result may be because of a floor effect driven by very low responding to the S− and its neighboring sounds in both groups.

Table 5. Distribution of BF for naive, vehicle-treated, and RGFP966-treated rats

BF (kHz)	Naive (127 sites, 5 rats)	VEH (192 sites, 8 rats)	RGFP966 (249 sites, 8 rats)
0.59–2.37	34.67%	36.45%	38.15%
3.36–13.45	41.73%	45.83%	42.57%
19.02–53.81	23.62%	17.71%	19.27%

This table displays the percentage of recording sites with a BF within ~2-octave bins for naive, vehicle (VEH)-treated, and RGFP966-treated rats.

Drug treatment groups did not differ on other performance metrics, including sound control measured by the percentage of responses to either AM sound versus responses during silent intertrial intervals (RGFP966: mean = 86.45, SE = 2.04; VEH: mean = 82.74, SE = 4.32; $t_{(14)} = -0.774$, $p = 0.451$) or number of bar presses to AM sounds (RGFP966: mean = 39.37, SE = 10.91; VEH: mean = 40.5, SE = 6.28; $t_{(14)} = 0.089$, $p = 0.930$). Therefore, the main effect of RGFP966 on the AM task was to increase memory specificity for the AM rate paired with reward (S+), adding to existing evidence that effects of HDAC3 inhibition on memory specificity can occur independently from effects on rate of learning (Rotondo and Bieszczad, 2020, 2021).

HDAC3 inhibition results in stimulus-specific and general plasticity effects in the primary auditory cortex

Memory for associations between specific sound features like a particular acoustic frequency and its link to potential for rewards, including the highly specific auditory memory enabled by HDAC3 inhibition, has been associated with signal-specific plasticity at the level of the A1 (Recanzone et al., 1993; Polley et al., 2006; Keeling et al., 2008; Bieszczad and Weinberger, 2010, 2012; Bieszczad et al., 2015; Shang et al., 2019; Rotondo and Bieszczad, 2020, 2021). Cortical representations of temporal features of sound can likewise be transformed by experience (Bao et al., 2004). Here, we sought to characterize changes in auditory cortical encoding of AM sounds associated with the behavioral specificity enabled by HDAC3 inhibition. Electrophysiological recordings in A1 were made following the AM rate memory test to compare A1 plasticity in the treated groups (RGFP966 vs vehicle) and the untreated naive control group on measures of phase-locking and response consistency. Although evoked responses to AM sounds do not significantly differ as a function of cortical frequency tuning (Bao et al., 2004), we note that the distribution of best frequency of cortical recording sites in vehicle- and RGFP966-treated rats did not differ from naive rats (vehicle vs naive: $\chi^2(2, 192) = 3.79$, $p = 0.149$; RGFP966 vs naive: $\chi^2(2, 249) = 2.91$, $p = 0.232$; Table 5). Thus, it is unlikely that frequency tuning properties of recording sites explain group differences in evoked responses to AM sounds.

Previous studies have reported a learning-induced increase in auditory cortical response consistency evoked by sound that generalizes across different sound stimuli, although these studies did not include an explicit behavioral test of memory specificity induced by the completion of training (Leon et al., 2008; Von Trapp et al., 2016). Thus, an open question is whether a cue-specific effect on cortical response variability might be associated with highly specific memory as presently observed in RGFP966-treated rats. Here, it was predicted that RGFP966-treated rats would have an increase in response consistency above and beyond the vehicle-treated counterparts and that this form of plasticity would be specific to the responses evoked by the remembered training sounds.

Table 6. Within-stimulus response consistency in naive, vehicle-treated, and RGFP966-treated animals

AM rate (Hz)	Naïve (127 sites, 5 rats)	VEH (192 sites, 8 rats)	RGFP966 (249 sites, 8 rats)
4.1	2409.75 ± 44.97	**2191.67 ± 23.20*** **	**2067.62 ± 20.38**§§**[a]
8.5	1299.61 ± 21.09	**1178.92 ± 14.74****	**1121.35 ± 11.65**§§**[b]
18.5	608.41 ± 10.54	**560.78 ± 7.36****	**530.94 ± 6.00**§§**[c]
40	279.78 ± 4.59	269.17 ± 3.58	266.99 ± 3.30
79	143.90 ± 2.87	**135.69 ± 1.80***	**132.83 ± 2.58***[d]
155	91.67 ± 2.05	**83.36 ± 1.33****	**78.49 ± 1.17**§§**[e]
307	65.14 ± 1.82	64.19 ± 0.13	62.99 ± 1.49
625	54.35 ± 1.77	49.37 ± 1.81	**45.21 ± 1.30***[f]

This table displays the sum of point-centroid distances determined by the kmeans clustering approach, a measure of within-stimulus response consistency. Note that smaller values indicate greater response consistency. Sample sizes are given in parentheses. All data are displayed as mean ± SE. Significant differences are in bold; *indicates a difference versus naive animals, *$p < 0.05$, **$p < 0.01$, ***$p < 0.001$; § indicates a difference versus vehicle (VEH)-treated animals, §§$p < 0.01$.

[a] One-way ANOVA: $F_{(2,565)} = 36.10$, $p = 0.0003$; Holm–Bonferroni-corrected two-tailed independent samples t test: naive versus VEH: $t_{(317)} = 4.70$, $p = 0.00,006$; naive versus RGFP966: $t_{(374)} = 8.00$, $p = 0.000003$; VEH versus RGFP966: $t_{(439)} = 4.06$, $p = 0.00,005$.

[b] One-way ANOVA: $F_{(2,565)} = 32.57$, $p = 0.0005$; Holm–Bonferroni-corrected two-tailed independent samples t test: naive versus VEH: $t_{(317)} = 4.80$, $p = 0.000004$; naive versus RGFP966: $t_{(374)} = 8.08$, $p = 0.000003$; VEH versus RGFP966: $t_{(439)} = 3.16$, $p = 0.0016$.

[c] One-way ANOVA: $F_{(2,565)} = 24.17$, $p = 0.0005$; Holm–Bonferroni-corrected two-tailed independent samples t test: naive versus VEH: $t_{(317)} = 3.81$, $p = 0.0002$; naive versus RGFP966: $t_{(374)} = 6.91$, $p = 0.00,003$; VEH versus RGFP966: $t_{(439)} = 3.21$, $p = 0.0028$.

[d] One-way ANOVA: $F_{(2,565)} = 4.54$, $p = 0.011$; Holm–Bonferroni-corrected two-tailed independent samples t test: naive versus VEH: $t_{(317)} = 2.54$, $p = 0.022$; naive versus RGFP966: $t_{(374)} = 2.69$, $p = 0.021$; VEH versus RGFP966: $t_{(439)} = 0.90$, $p = 0.367$.

[e] One-way ANOVA: $F_{(2,565)} = 19.01$, $p = 0.0005$; Holm–Bonferroni-corrected two-tailed independent samples t test: naive versus VEH: $t_{(317)} = 3.55$, 0.0008; naive versus RGFP966: $t_{(374)} = 5.99$, $p = 0.00,003$; VEH versus RGFP966: $t_{(439)} = 2.74$, $p = 0.006$.

[f] One-way ANOVA: $F_{(2,565)} = 7.48$, $p = 0.001$; Holm–Bonferroni-corrected two-tailed independent samples t test: naive versus VEH: $t_{(317)} = 1.87$, $p = 0.106$; naive versus RGFP966: $t_{(374)} = 4.14$, $p = 0.00,004$; VEH versus RGFP966: $t_{(439)} = 1.94$, $p = 0.106$.

To determine AM-noise-evoked response consistency in A1, we calculated the sum of point-to-centroid distances using a k-means clustering approach. Here, lower values mean greater response consistency (i.e., lower response variability). There was a significant effect of training: vehicle- and RGFP966-treated rats exhibited a significant increase in response consistency for nearly all stimuli (Table 6; Fig. 6). In support of our prediction, RGFP966-treated rats had greater response consistency than vehicle-treated rats. However, this effect was observed for nearly all stimuli. To confirm this result was not influenced by the uneven number of data points between groups, we also performed a bootstrapping analysis using 40 samples to equally subsample the data per group over 10,000 iterations to determine a 98.75% confidence interval from the resulting distribution. This analysis revealed the same results, that is, both trained groups exhibited increased response consistency relative to naive rats, with RGFP966-treated rats exhibiting greater response consistency than vehicle-treated rats. Together, this suggests that changes in response consistency represent a generalized change in cortical sound processing that is induced by training and is facilitated by HDAC3 inhibition.

Previous studies have reported learning-induced increases in the magnitude of phase-locked cortical activity, with some indirect evidence that changes in phase locking may be stimulus specific (Beitel et al., 2003; Bao et al., 2004). To determine the strength of phase locking, we calculated for each recording site within A1, a VS and the RS, the latter of which estimates the significance of VS, controlling for the total number of spikes. At the cortical level of A1, the ceiling rates for phase locking are substantially lower relative to brain structures closer to the periphery, which can follower faster rates of modulated sound (Joris et al., 2004). In anesthetized preparations, auditory cortical phase locking is typically limited to

AM rates below 20–30 Hz (Eggermont, 1991; Miller et al., 2002; Bao et al., 2004; Anderson et al., 2006; Fitzpatrick et al., 2009). Therefore, these analyses were restricted to a set of slower AM test rates: 4.1, 8.5, and 18.5 Hz (the S+).

Results for the phase-locking analyses differed from the response consistency analysis in two major ways. First, RGFP966-treated but not vehicle-treated animals showed learning-induced changes in phase locking (Fig. 7; Table 7). Because both vehicle- and RGFP966-treated animals were able to learn the task equally, the differences in learning-induced phase locking suggests that plasticity in cortical phase locking may underlie a behavioral function beyond task acquisition that relates to the quality of the memory formed by learning (e.g., such as the specificity or strength of the memory). Second, changes in phase locking exhibited a greater degree of stimulus specificity than response consistency. RGFP966-treated rats, compared with naive or vehicle-treated rats, showed a significant increase in vector strength in responses evoked by the rewarded (S+) 18.5 Hz AM rate but no changes in responses evoked by the novel 4.1 and 8.5 Hz AM rates. Together, this pattern of changes suggests a selective enhancement in phase-locked responses to the behaviorally relevant 18.5 Hz rate.

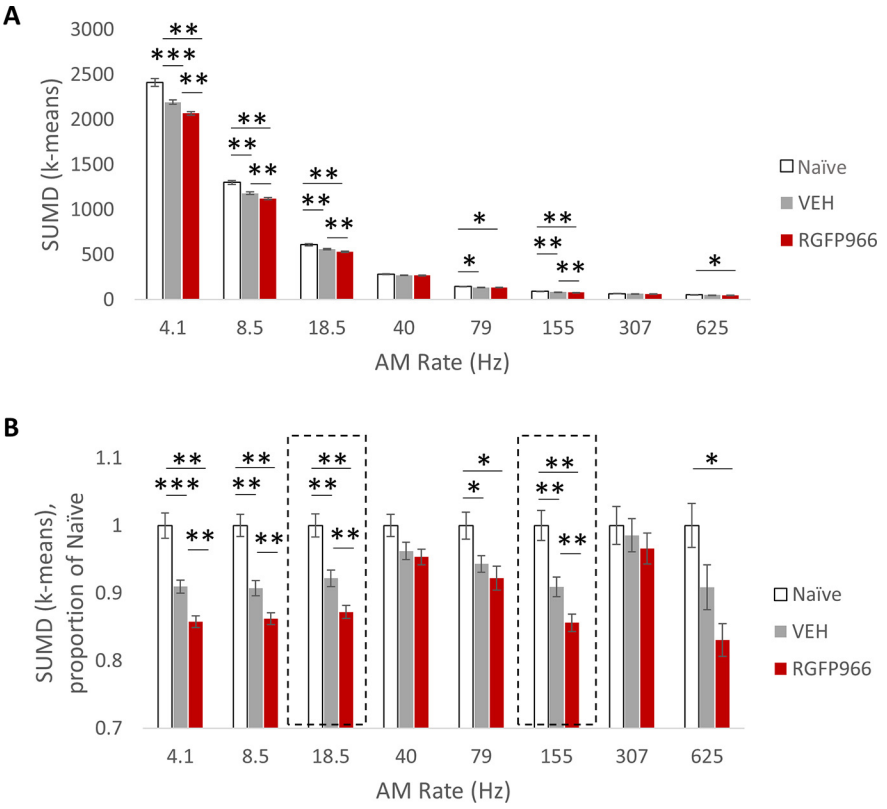

Figure 6. A1 response consistency is increased as a function of memory formation and of HDAC3i-enabled memory specificity. ***A***, ***B***, The raw SUMD (***A***) and (***B***) the sum of SUMD as a proportion of naive subjects. Response consistency increased with training, revealed by the lower SUMD in vehicle (VEH)-treated and RGFP966-treated groups. Further, RGFP966-treated rats had greater response consistency than vehicle-treated rats. These effects generalized across most AM rates. Data is displayed as mean ± SE. *$p < 0.05$, **$p < 0.01$, ***$p < 0.001$.

To further investigate these changes in cortical phase locking, we next determined the proportion of cortical recordings sites that exhibited significantly phase-locked responses for each AM rate, using the criteria of a Rayleigh statistic ≥5.991, which represents a $p = 0.05$ threshold value (Table 8; Fig. 8*A*). RGFP966-treated rats exhibited an increased proportion of sites with significant phase locking to the 18.5 Hz AM rate (0.630/157 of 249 cites), versus naive rats (0.440; 56 of 127 sites). In contrast, both RGFP966- (0.698; 174 of 249 sites) and vehicle-treated (0.687; 132 of 192 sites) rats exhibited a decreased proportion of sites with significant phase locking to the 4.1 Hz AM rate versus naive rats (0.748; 95 of 127 sites). This pattern of changes may also reflect competitive loss (here, an increase in metabolic resources dedicated to representing behavioral relevant sounds at the expense of novel, distinct sounds), especially when behaviorally relevant sounds with enhanced phase locking are near the ceiling of cortical phase-locking ability (i.e., 20–30 Hz; Bao et al., 2004). We next tested whether group differences in phase-locking strength would still be observed after removing the sites with no significant phase-locked response. Even when only considering sites with significantly phase-locked responses, RGFP966-treated rats still had greater vector strength in responses evoked by the rewarded 18.5 Hz AM rate (Fig. 9*B*; Table 8). Therefore, RGFP966-treated rats exhibit at least two distinct forms of signal-specific plasticity related to phase locking: (1) a change in the proportion of phase-locked sites and (2) a change in the strength of phase locking both overall and within just the significantly phase-locked sites.

Overall, there is a complex pattern of cortical changes that occur with learning about AM sounds that may be modified by the level of specificity with which long-term memory is formed. Response consistency for most AM rates is improved with training, with more pronounced effects in the HDAC3-inhibited group versus the vehicle-treated group. Interestingly, there is a significant relationship between response consistency and the Rayleigh statistic (18.5 Hz: $n = 568$, $r = -0.269$, $p <$0.00,001; 8.5 Hz: $n = 568$, $r = -0.275$, p = <0.00,001; 4.1 Hz: $n = 568$, $r = -0.079$, $p = 0.059$), suggesting that better response consistency may facilitate significant phase locking as has been previously proposed (White-Schwoch et al., 2017). However, because better response consistency was also found in instances without corresponding enhancements in phase locking at the group level (as in responses evoked by 4.1 Hz in the vehicle- and RGFP966-treated groups), there does not appear to be a causal relationship between response consistency and the strength of phase locking. Nonetheless, all observed forms of plasticity are more likely to occur with HDAC3 treatment and the formation of highly specific memory. Importantly, the plasticity related to phase-locking measures, but not response consistency measures, was signal specific.

HDAC3 inhibition enhances response magnitude of FFRs evoked by the rewarded AM rate

To follow up on our finding of signal-specific changes in phase locking in HDAC3-inhibited rats, we also analyzed the FFR, a noninvasive recording of neural activity that is phase locked to

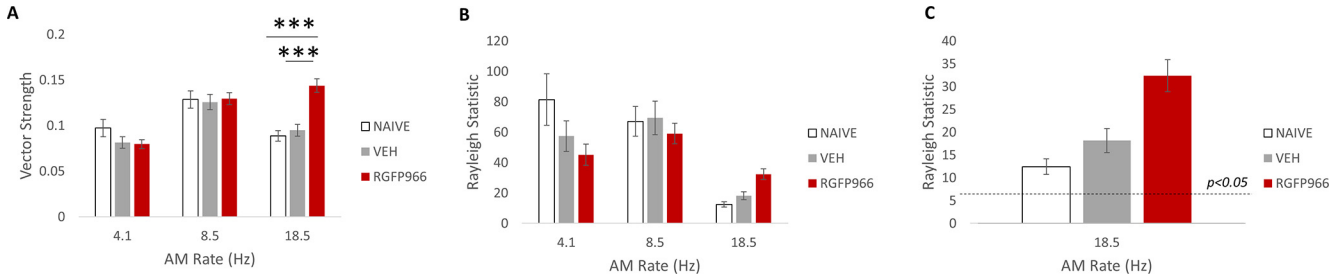

Figure 7. HDAC3 inhibition enhances A1 phase-locking to the rewarded AM rate. ***A***, Vector strength, a measure of phase-locking strength, is significantly greater in responses evoked by the rewarded 18.5 Hz AM rate among RGFP966-treated animals versus naive and vehicle (VEH)-treated animals. ***B***, The Rayleigh statistic estimates the significance of phase-locking, where a value of 5.991 corresponds to $p < 0.05$ and a value of 13.816 corresponds to $p < 0.001$. ***C***, A zoomed-in view of the Rayleigh statistics for responses evoked by the rewarded 18.5 Hz AM rate. Data are presented as mean ± SE. The dashed line represents the threshold value for significant phase locking.

Table 7. Vector strength and Rayleigh statistic in naive, vehicle-treated, and HDAC3-treated animals

	AM rate (Hz)	Naive (127 sites, 5 rats)	VEH (192 sites, 8 rats)	RGFP966 (249 sites, 8 rats)
VS	4.1	0.09 ± 0.009	0.08 ± 0.006	0.08 ± 0.004
	8.5	0.12 ± 0.009	0.12 ± 0.008	0.13 ± 0.006
	18.5	0.08 ± 0.005	0.09 ± 0.006	**0.14 ± 0.007*****§§§**[a]**
RS	4.1	81.40 ± 16.929	57.38 ± 10.138	45.10 ± 6.959
	8.5	67.13 ± 9.776	69.39 ± 11.018	59.05 ± 6.754
	18.5	12.43 ± 1.699	18.56 ± 2.660	32.35 ± 3.509

This table displays VS and the RS, which estimates the significance of VS taking into account the total number of spikes. Sample sizes are given in parentheses. All data are displayed as mean ± SE. For VS data, significant differences are in bold; * indicates a difference versus naive animals, ***$p < 0.001$. § indicates a difference versus vehicle (VEH)-treated animals, §§§$p < 0.001$ for RS data; the critical values are 5.991 for $\alpha = 0.05$ and 13.816 for $\alpha = 0.001$.

[a]One-way ANOVA: $F_{(2,565)} = 19.614$, $p = 0.0001$; Holm–Bonferroni-corrected two-tailed independent samples t test: naive versus VEH: $t_{(317)} = 0.673$, $p = 0.502$; naive versus RGFP966: $t_{(374)} = -4.964$, $p = 0.0006$; VEH versus RGFP966: $t_{(439)} = -4.865$, $p = 0.0004$.

periodic features of sound, including amplitude modulation. The FFR provides two distinct opportunities relative to our intracortical recordings. First, the FFR may reflect both cortical and subcortical response components depending on the characteristics of the sounds used to evoke it (Coffey et al., 2016). Importantly, subcortical structures can phase lock to much faster modulation rates than the cortex, allowing us to quantify phase locking to the faster unrewarded 155 Hz AM rate used in the present study. Under these conditions, we assume that FFRs evoked by the 18.5 Hz AM sound have both cortical and subcortical components, whereas FFRs evoked by the remaining faster sound set (40, 79, and 155 Hz) are primarily of subcortical origin. Second, because the FFR is noninvasive, we can collect responses at multiple time points to determine experience-dependent effects using a within-subjects design. Indeed, previous work in humans has shown that the FFR may change with experience in a way that is selective for behaviorally relevant sounds (Song et al., 2008; Strait et al., 2012). The present study recorded AM noise-evoked FFRs (1) before tone–tone discrimination training, (2) after tone–tone discrimination training, and (3) after AM rate discrimination training. Over the AM rate discrimination training phase interval, it was predicted that memory specific to AM rate would be associated with changes in the FFR that were selective to the behaviorally relevant AM rates.

Importantly, characteristics of AM-evoked FFRs, including response magnitude, response consistency, and timing jitter, were stable over weeks throughout the course of tone–tone discrimination training (Table 9, Fig. 9*C*). In addition, there were no differences in the change in these response characteristics between the subsequent drug treatment groups (Table 9). This suggests that in absence of experience of AM sounds, the representation of AM is stable. In contrast, over the course of AM rate discrimination training, there was a significant increase in response magnitude in FFRs evoked by the rewarded 18.5 Hz AM rate but only in the RGFP966-treated group (Table 9, Fig. 9*D*). There were no changes in response magnitude in FFRs evoked by any other AM rate, including the unrewarded 155 Hz AM rate. Response consistency and timing jitter were stable over the course of AM rate discrimination training (Table 9). Collectively, the FFR validates the intracortical results in that there is sound-selective enhancement in phase locking because of learning about the rewarded 18.5 Hz AM rate, with effects on phase locking most prominent under conditions of HDAC3 inhibition that enabled highly sound-specific memory.

A surprising result was the lack of significant changes in phase locking to the unrewarded 155 Hz AM rate. However, this result mirrors the observed behavioral patterns in which specificity effects were driven by increased selectivity to the rewarded 18.5 Hz AM rate, rather than a concomitant selective decrease in behavioral responding to the unrewarded 155 Hz AM rate. The lack of significant neural changes to 155 Hz could be a reflection of the behavioral strategy of the animal to respond more to the S+ (18.5 Hz) without taking into account the specific identity of the S−. Thus, together with the intracortical recordings, we predicted that the cue-selective changes in phase locking could be a substrate of memory specificity for AM rate.

Auditory system plasticity is correlated with individual differences in memory specificity

To investigate forms of signal-specific auditory plasticity that serve as substrates of memory specificity for AM rate, we pursued correlations between neural measures sensitive to phase locking and behavioral measures that index memory specificity. Although there were multiple potential indices of memory specificity, we focused on the percentage of responses to the 18.5 Hz S+ during the memory test for several reasons. First, memory specificity effects were largely driven by differences in responding to the S+, as opposed to the S−, as discussed above (Fig. 5; Table 4). Further, the percentage of responses to the S+ is a straightforward metric that is strongly correlated with other specificity indices (% bar presses to S+ vs Δ % bar presses to S+ vs S−: $r = 0.981$, $p < 0.00{,}001$; vs Δ % bar presses to S+ vs nearby neighbors: $r = 0.987$, $p < 0.00{,}001$; vs Δ % bar presses to S+ vs distant neighbors: $r = 0.976$, $p < 0.00{,}001$).

It was first important to understand whether the magnitude of phase-locked neural activity measured in the FFR was

Table 8. Vector strength in cortical sites with significant phase locking in naive, vehicle-treated, and HDAC3-treated animals

	AM rate (Hz)	Naive (127 sites, 5 rats)	VEH (192 sites, 8 rats)	RGFP966 (249 sites, 8 rats)
Proportion with significant RS	4.1	0.748	**0.687***[a]	**0.698***[b]
	8.5	0.795	**0.740****[c]	0.819
	18.5	0.440	0.421	**0.630*****[d]
VS (sites with significant RS)	4.1	0.12 ± 0.011	0.11 ± 0.009	0.10 ± 0.005
	8.5	0.15 ± 0.011	0.16 ± 0.009	0.15 ± 0.007
	18.5	0.14 ± 0.006	0.17 ± 0.010	**0.20 ± 0.008*****[e]

This table shows the proportion of cortical sites with significant phase locking ($p < 0.05$), as revealed by an RS value of at least 5.991. VS for sites with significant phase locking is displayed (mean ± SE). Significant differences are in bold; *indicates a difference versus naive animals, *$p < 0.05$, **$p < 0.01$, ***$p < 0.001$; § indicates a difference versus vehicle (VEH)-treated animals, §$p < 0.05$.
[a] Binomial test, $p = 0.034$.
[b] Binomial test, $p = 0.045$.
[c] Binomial test, $p = 0.037$.
[d] Binomial test, $p < 0.0001$.
[e] One-way ANOVA: $F_{(2,293)} = 8.398$, $p = 0.0003$; Holm–Bonferroni-corrected two-tailed independent samples t test: naive versus VEH: $t_{(135)} = -1.915$, $p = 0.058$; naive versus RGFP966: $t_{(161)} = -3.802$, $p = 0.0009$; VEH versus RGFP966: $t_{(181)} = -2.252$, $p = 0.050$.

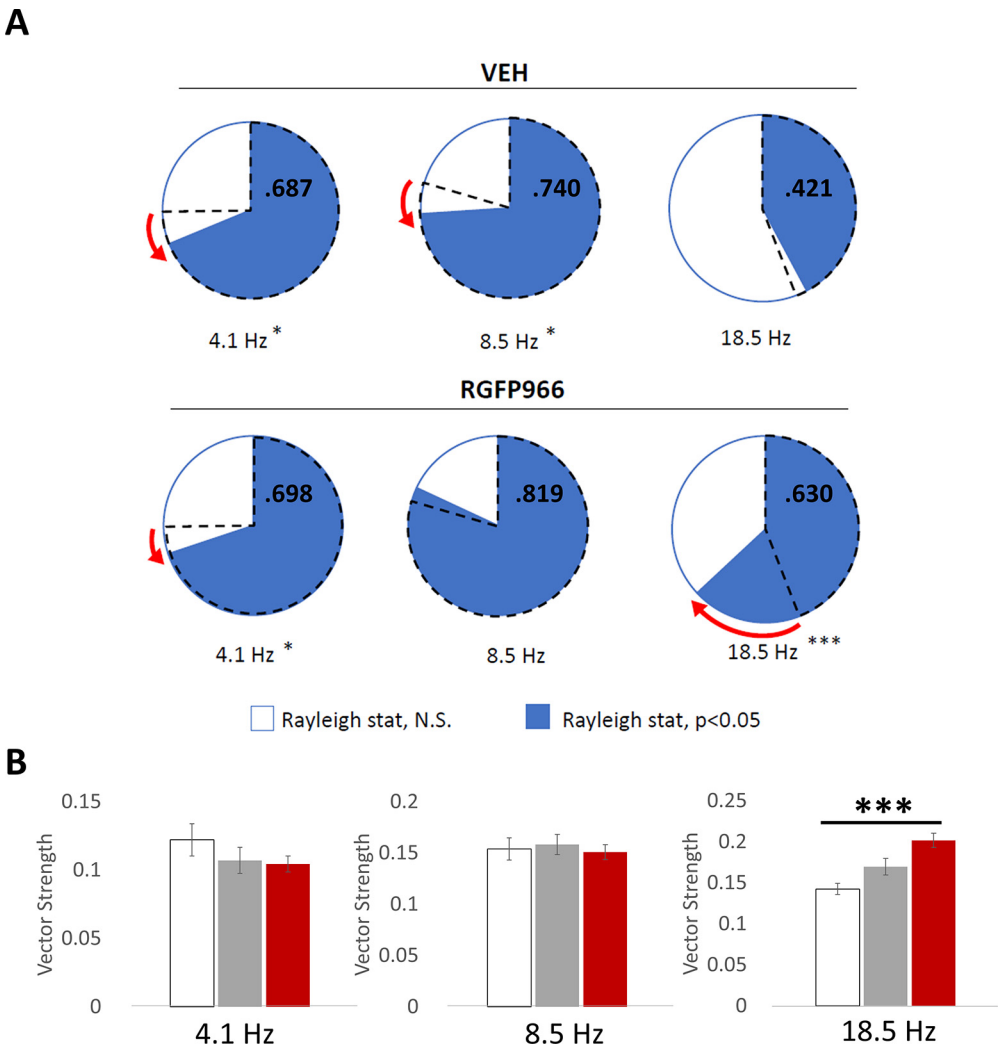

Figure 8. HDAC3 inhibition increases the proportion of cortical sites that phase locked to the rewarded 18.5 Hz AM rate and the strength of phase locking within those sites. ***A***, Pie charts display the proportion of recording sites in A1 in vehicle (VEH)-treated and RGFP966-treated animals with a Rayleigh statistic ≥5.991, which corresponds to $p < 0.05$. The dashed lines represent the proportion of cortical sites with significant phase-locked responses in naive animals. Red arrows represent the direction of significant changes. *$p < 0.05$ vs. naive, ***$p < 0.001$ versus naive. ***B***, When only considering cortical sites with a Rayleigh statistic ≥5.991, RGFP966-treated animals have significantly greater vector strength in responses evoked by the rewarded 18.5 Hz versus naive rats. Data are presented as mean ± SE. *$p < 0.05$.

correlated with phase-locked activity measured in the auditory cortex. As noted previously (Frequency following response recordings), FFRs evoked by the 18.5 Hz S+ likely include a significant cortical component in addition to subcortical components. Although the FFR does not exclude the possibility of reflecting subcortical plasticity, we cannot with these data alone tease apart cortically versus subcortically sourced components of the FFR. Nonetheless, the learning-induced change in

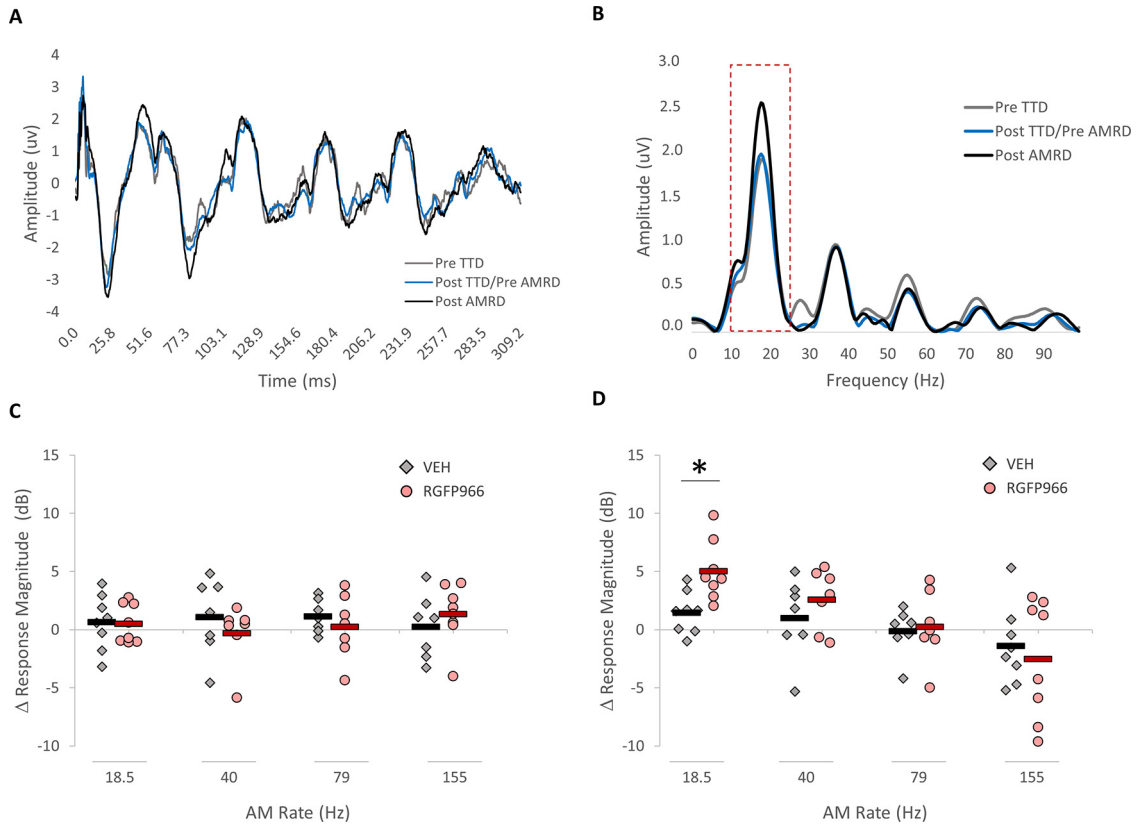

Figure 9. HDAC3 inhibition results in enhanced FFR response magnitude that is selective to the rewarded AM rate. ***A***, A representative FFR trace evoked by 18.5 Hz AM noise at the pretone discrimination training, post-tone discrimination training, and post-AM-rate discrimination training time points in an RGFP966-treated rat. ***B***, A fast Fourier transform of the FFR shown (***A***) reveals stronger encoding of the 18.5 Hz AM rate following AM rate discrimination training. ***C***, Over the course of tone–tone discrimination leaning, response magnitude is stable in AM noise-evoked FFRs. ***D***, Over the course of AM rate discrimination learning, RGFP966-treated rats show a selective increase in response magnitude of FFRs evoked by the rewarded 18.5 Hz S+ ($p < 0.01$), and a greater increase versus vehicle (VEH)-treated rats. There were no other significant changes in response magnitude or drug treatment group differences. Dots in ***C***,***D*** represent individual data points while the bars represent the mean. *$p < 0.05$ versus vehicle.

Table 9. Changes in AM noise-evoked FFRs in vehicle- and HDAC3-treated animals

		Δ TTD		Δ AMRD	
	AM rate (Hz)	VEH	RGFP966	VEH	RGFP966
Mag (dB)	18.5	0.65 ± 0.85 (8)	0.50 ± 0.59 (8)	1.45 ± 0.63 (8)	**5.03 ± 0.90**∗§§[a] (8)
	40	1.08 ± 1.25 (7)	−0.29 ± 0.96 (7)	1.00 ± 1.29 (7)	2.58 ± 0.98 (7)
	79	1.14 ± 0.54 (7)	0.25 ± 1.04 (7)	−0.12 ± 0.75 (7)	0.24 ± 1.15 (7)
	155	0.26 ± 1.04 (7)	1.34 ± 0.90 (8)	−1.38 ± 1.19 (8)	−2.51 ± 1.80 (8)
Con (Fisher *z*)	18.5	0.04 ± 0.09 (8)	0.09 ± 0.08 (8)	0.03 ± 0.06 (8)	0.11 ± 0.05 (8)
	40	0.12 ± 0.08 (7)	0.14 ± 0.19 (7)	−0.01 ± 0.05 (7)	−0.03 ± 0.12 (7)
	79	0.01 ± 0.06 (7)	−0.02 ± 0.10 (7)	0.13 ± 0.10 (7)	0.02 ± 0.11 (7)
	155	0.11 ± 0.07 (7)	0.02 ± 0.21 (8)	−0.14 ± 0.10 (8)	−0.19 ± 0.29 (8)
Jitter (ms)	18.5	0.00 ± 0.02 (8)	0.01 ± 0.29 (8)	−0.026 ± 0.04 (8)	−0.04 ± 0.03 (7)
	40	−0.01 ± 0.03 (7)	−0.02 ± 0.23 (7)	0.01 ± 0.03 (7)	0.01 ± 0.023 (7)
	79	0.03 ± 0.03 (7)	0.01 ± 0.02 (7)	−0.01 ± 0.03 (7)	0.00 ± 0.02 (7)
	155	−0.02 ± 0.02 (7)	−0.01 ± 0.019 (8)	0.01 ± 0.01 (8)	0.02 ± 0.02 (8)

This table displays the change in FFR response magnitude (mag.), response consistency (con.), and timing jitter over the course of tone–tone discrimination training and over the course of AM rate discrimination training. All data are displayed as mean ± SE, with sample sizes in parentheses. Significant differences are in bold; ∗ indicates a difference from 0 (i.e., no change), *$p < 0.05$; § indicates a difference versus vehicle (VEH)-treated animals, §§$p < 0.01$. TTD; Tone–tone discrimination; Mag, Response magnitude; Con, response consistency.

[a] Holm–Bonferroni-corrected one-sample *t* test: $t_{(7)} = 4.69$, $p = 0.003$; Holm–Bonferroni independent samples *t* test (vs VEH): $t_{(14)} = 3.22 = 0.024$.

FFR response magnitude was significantly correlated with phase-locking strength in the auditory cortical recordings, which validates the use of FFR as a window into cortical processes (Fig. 10*A*; Table 10). As such, it is therefore not surprising that the strength of phase locking in responses evoked by 18.5 Hz, whether measured from the FFRs (Fig. 10*B*; Table 10) or from cortical recordings (Fig. 10*C*, *D*; Table 10) was associated with a greater degree of memory specificity at the level of behavior.

Discussion

We report a novel role for HDAC3i to enhance behavioral memory specificity for a temporal feature of sound, the AM rate. HDAC3i enabled greater memory specificity produced by several learning-induced forms of neurophysiological plasticity in the A1. Unlike vehicle-treated rats, rats treated with an HDAC3 inhibitor exhibited an increase in the magnitude of phase locking that was specific to the rewarded AM rate—an effect that was

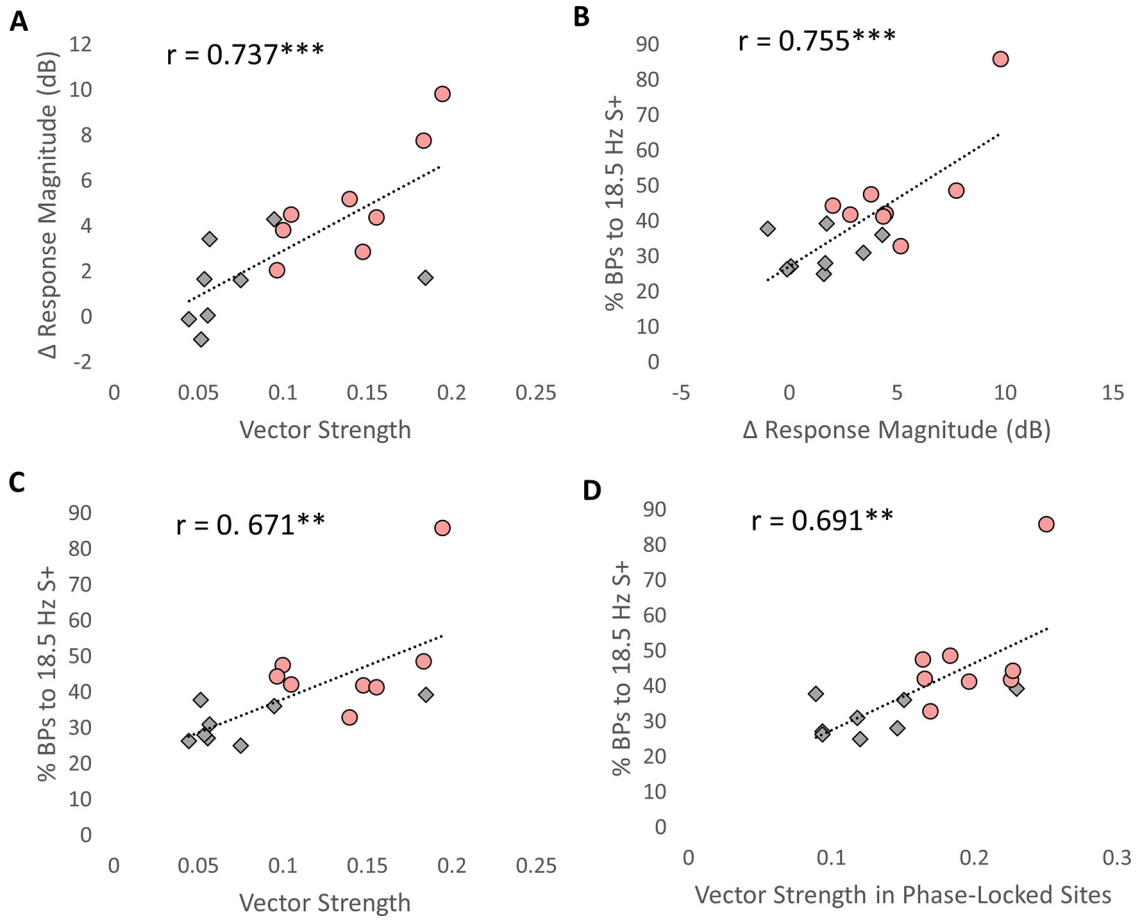

Figure 10. Auditory system plasticity is correlated with AM-rate specific memory. ***A–D*** present correlative data between several different types of measures: auditory cortical phase locking to the 18.5 Hz AM rate (vector strength), learning-induced change in FFR response magnitude evoked by the 18.5 Hz AM rate, and the percentage of bar presses (% BPs) to the 18.5 Hz S+ during the AM rate memory test. ***A***, Greater A1 phase locking to 18.5 Hz is related to greater increases in FFR response magnitude to 18.5 Hz. ***B***, A greater increase in response magnitude in FFRs by the 18.5 Hz S+ is related to a to a greater degree of memory specificity, as indexed by the percentage of bar presses (% BPs) to 18.5 Hz S+ during the AM rate memory test. ***C***, ***D***, Stronger auditory cortical phase locking, when considering all recording sites in A1 (***C***) or only responses from phase-locked sites (***D***) are also related to a greater degree of memory specificity. Gray diamond markers represent vehicle-treated rats while pink circle markers represent RGFP966-treated rats.

Table 10. Summary of correlations with phase-locked neural responses and sound-cued behavior

	All (n = 16)	VEH (n = 8)	RGFP966 (n = 8)
VS versus Δ Resp. Mag.	**0.737****	0.305	**0.814***
RS versus Δ Resp. Mag.	**0.700****	0.226	0.668
VS versus % bar presses to S+	**0.671****	0.619	0.555
RS versus % bar presses to S+	**0.764*****	0.618	**0.787***
% Phase-locked sites versus % bar presses	**0.525***	0.626	0.192
VS (for phase-locked sites) versus % bar presses	**0.691****	0.533	0.637
Δ Resp. Mag. versus % bar presses	**0.755*****	0.156	**0.740***

This table displays the Pearson r values for correlations between phase-locked neural responses measured from the scalp with the FFR (response magnitude) or recorded extracellularly from A1 (VS, RS, % of phase-locked sites) and the percentage of responses to the rewarded 18.5 Hz AM rate (% bar presses to S+) during the AM rate memory test). Resp. Mag., Response magnitude. Δ Resp. Mag refers to the difference in FFR response magnitude pre- to post-AM-rate discrimination training. Sample sizes are in parentheses. Significant correlations are in bold. *$p < 0.05$, **$p < 0.01$, ***$p < 0.001$.

also validated by AM-rate-specific effects in the surface recorded FFR. HDAC3 inhibition also caused a larger increase in A1 response consistency (relative to vehicle) that generalized across responses evoked by a range of AM stimuli. Further analysis that removed sites without significant phase locking revealed that the cortical increase in sound-specific phase locking was attributable to both an increase in the proportion of sites that participated in the phase-locked response and a concomitant increase in the strength of phase locking among these sites. Brain–behavior relationships revealed that measures of phase locking correlated with individual differences in behavioral memory specificity among all rats, regardless of treatment. In sum, these findings support that the effect of HDAC3i to enhance memory specificity is mediated by enabling signal-specific auditory neuroplasticity. The findings extend this hypothesis to memory formation for temporal features of sounds with temporal coding strategies in the auditory brain.

HDAC3 inhibition enhances temporal coding of the rewarded sound

Temporal coding via phase locking to sound features can increase the precision of sound-evoked neural activity for behaviorally relevant information (Lakatos et al., 2008; Schroeder et al., 2010; Peelle et al., 2013). Here, we report an increase in the strength of phase locking to the rewarded AM rate in the primary auditory cortex among rats with highly specific memory. Notably, when considering only recording sites with significant phase-locked responses, the pattern of effects with respect to the strength of phase-locking hold; rats treated with the HDAC3 inhibitor exhibit enhanced phase locking to the rewarded AM rate. This suggests that the highly

specific memory for AM rate entails both a change in the neurons that are recruited into the response and a change in the response characteristics within neurons (Bao et al., 2004). Signal-specific enhancement of cortical phase locking is in line with findings that phase locking is shaped by both acoustic information and other nonsensory and experience-dependent information such as meaning (Bao et al., 2004; Strait et al., 2012; Peelle et al., 2013). Here, we report that individual differences in the strength of phase locking were significantly correlated with the degree of memory specificity for the rewarded sound, regardless of treatment.

Enhanced cortical phase locking to the rewarded AM rate in extracellular cortical recordings was validated by the FFR, a signal with both cortical and subcortical components (Coffey et al., 2016). Indeed, measures of the magnitude of phase-locked activity in the FFR with magnitude of phase-locked activity in the primary auditory cortex were significantly positively correlated. Nonetheless, the FFR was recorded longitudinally and revealed that phase locking is enhanced within individual subjects over the course of learning about AM sounds, and even more so in animals with highly specific memory for the rewarded AM sound.

Interestingly, the FFR did not reveal a significant change in phase locking evoked by the explicitly unrewarded AM sound (155 Hz), although this rate is within the range of subcortical phase-locking ability (Joris et al., 2004; Fitzpatrick et al., 2009; Coffey et al., 2016). It is possible that this form of plasticity is not readily induced at the subcortical level. Alternatively, it may be that plasticity is driven more strongly by rewarded sounds. Future studies in which a faster AM rate is explicitly rewarded may find that HDAC3 inhibition will facilitate encoding of behaviorally relevant sensory details, regardless of the features. A second alternative takes into account that 18.5 Hz and 155 Hz are on different sides of a perceptual barrier in that modulations at 18.5 Hz are perceived as flutter, and modulations at 155 Hz are perceived as roughness (Besser, 1967; Krumbholz et al., 2000). Thus, animals could use the sound quality, rather than specific differences in AM rate, to guide their behavioral responses. Indeed, this is consistent with the pattern of results observed in the vehicle-treated group, which displayed an observable degree of memory specificity despite not showing any significant enhancements in phase locking. If true, then it is notable that treatment with HDAC3i may bias subjects to encode specific features of the stimulus even when they are not strictly necessary to solve the task (i.e., as other strategies could have been used), as has been suggested by previous results (Bieszczad et al., 2015; Rotondo and Bieszczad, 2020, 2021).

HDAC3 inhibition enhances the learning-induced increase in auditory cortical response consistency to AM sounds

In contrast to the signal-specific changes in phase locking, we observed another form of plasticity with a temporal component that instead generalized across all AM sounds tested. Specifically, we observed an increase in sound-evoked response consistency (i.e., a decrease in response variability) in the primary auditory cortex in both trained groups, with a significantly greater increase in rats treated with the HDAC3 inhibitor. That auditory training improves auditory response consistency, even for sounds that were not explicitly trained, is in line with previous studies (Leon et al., 2008; Hornickel et al., 2012; Anderson et al., 2013).

Many studies have correlated auditory-evoked response consistency with proficiency in auditory and language skills (Anderson et al., 2012; Hornickel and Kraus, 2013; Von Trapp et al., 2016; White-Schwoch et al., 2017; Caras and Sanes,2019). Thus, one interpretation of these data are that response consistency facilitates learning within the AM category as it could provide a foundation of consistently discriminable neural representations of acoustically similar sounds that enables behavioral discrimination. Indeed, subjects with the best response consistency also had enhancements in phase locking and a greater degree of memory specificity, although these measures were not consistently correlated. Future analyses will consider the potential interactive contribution of these forms of plasticity to learned behavior.

As with phase locking, response consistency may be improved with attention or task engagement (Von Trapp et al., 2016). However, these factors are not a prerequisite as other studies, including the present one, have observed improved response consistency in the absence of attentional or contextual factors (Leon et al., 2008) or active task engagement (Hornickel et al., 2012; Anderson et al., 2013). Given that HDAC3 inhibition enhanced response consistency above and beyond the level of vehicle-treated controls, and that these effects were observed ~3 d after the final auditory training session and weeks after the last injection of RGFP966, these are evidently long-lasting systems-level effects that are likely driven by stable changes in gene expression and cellular function initiated by an HDAC3-dependent mechanism. Several key genes have been implicated in auditory cortical (Centanni et al., 2014) and subcortical (Selinger et al., 2016) temporal response consistency. Inhibiting HDAC3 during an active memory consolidation process may facilitate, amplify, or prolong expression of learning-induced genes critical to the faithful temporal encoding of sounds at a cellular level of activity-dependent physiological plasticity in the auditory circuit. This effect could be inherited at the systems level to enhance a select population response (e.g., more cells with better temporal coding for a learned behaviorally significant sound), which in turn would be expressed at the behavioral level as a greater degree of specificity in sound-cued responding to the remembered versus novel stimuli. An important future direction is to determine the underlying molecular substrates regulated by HDAC3 to produce this cascade of neurophysiological and behavioral effects. Candidates known to be regulated by HDAC3 include GABAergic and serotonergic signaling machinery (Zhou et al.,2019; Nakamura et al., 2020), implicated in modifying both phase locking and frequency tuning curves in the auditory system (Gonzalez-Burgos and Lewis, 2008; Zhang et al., 2016; Askew et al., 2017; Kato et al., 2017).

In sum, epigenetic manipulations, like HDAC inhibition, can support the formation of highly specific memory for temporal features of sound. For the first time we demonstrate that inhibiting HDAC3 can alter temporal coding of sound features in the auditory brain. Like memory specific to acoustic frequency, memory specific to AM rate is supported by signal-specific patterns of neurophysiological change that provide discriminable representations of behaviorally relevant sound features. The susceptibility of these neurophysiological changes to HDAC3 regulation can help leave a lasting physiological impression of past activity regardless of the stimuli evoking those patterns of responses or the neural coding strategy (Bieszczad et al., 2015; Rotondo and Bieszczad, 2020, 2021). Collectively, this work supports that epigenetic regulators like HDACs play an important role in the development of precise representations of spectral and temporal features of sound, both of which

are critical for communication skills. More broadly, it supports a hypothesis in which HDAC inhibitors can target and transform detailed in-the-moment sensory information into long-term storage in memory, regardless of the type of experience, stimulus, or the way it is encoded in the brain (Bieszczad et al., 2015; Phan and Bieszczad, 2016).

References

Anderson S, Parbery-Clark A, Yi HG, Kraus N (2011) A neural basis of speech-in-noise perception in older adults. Ear Hear 32:750–757.

Anderson S, Parbery-Clark A, White-Schwoch T, Kraus N (2012) Aging affects neural precision of speech encoding. J Neurosci 32:14156–14164.

Anderson S, White-Schwoch T, Parbery-Clark A, Kraus N (2013) Reversal of age-related neural timing delays with training. Proc Natl Acad Sci U S A 110:4357–4362.

Anderson SE, Kilgard MP, Sloan AM, Rennaker RL (2006) Response to broadband repetitive stimuli in auditory cortex of the unanesthetized rat. Hear Res 213:107–117.

Askew C, Intskirveli I, Metherate R (2017) Systemic nicotine increases gain and narrows receptive fields in A1 via integrated cortical and subcortical actions. eNEURO 4:ENEURO.0192–17.2017.

Bao S, Chang EF, Woods J, Merzenich MM (2004) Temporal plasticity in the primary auditory cortex induced by operant perceptual learning. Nat Neurosci 7:974–981.

Beitel RE, Schreiner CE, Cheung SW, Wang X, Merzenich M (2003) Reward-dependent plasticity in the primary auditory cortex of adult monkeys trained to discriminate temporally modulated signals. Proc Natl Acad Sci U S A 100:11070–11075.

Besser GM (1967) Some physiological characteristics of auditory flutter fusion in man. Nature 214:17–19.

Bieszczad KM, Weinberger NM (2010) Representational gain in cortical area underlies increase of memory strength. Proc Natl Acad Sci U S A 107:3793–3798.

Bieszczad KM, Weinberger NM (2012) Extinction reveals that primary sensory cortex predicts reinforcement outcome. European J Neurosci 35:598–613.

Bieszczad KM, Bechay K, Rusche JR, Jacques V, Kudugunti S, Miao W, Weinberger NM, McGaugh JL, Wood MA (2015) Histone deacetylase inhibition via RGFP966 releases the brakes on sensory cortical plasticity and the specificity of memory formation. J Neurosci 35:13124–13132.

Campbell RR, Wood MA (2019) How the epigenome integrates information and reshapes the synapse. Nat Rev Neurosci 20:133–147.

Caras ML, Sanes DH (2019) Neural variability limits adolescent skill learning. J Neurosci 39:2889–2902.

Centanni TM, Booker AB, Sloan AM, Chen F, Maher BJ, Carraway RS, Khodaparast N, Rennaker R, LoTurco JJ, Kilgard MP (2014) Knockdown of the dyslexia-associated gene Kiaa0319 impairs temporal responses to speech stimuli in rat primary auditory cortex. Cereb Cortex 24:1753–1766.

Coffey EB, Herholz SC, Chepesiuk AM, Baillet S, Zatorre RJ (2016) Cortical contributions to the auditory frequency following response revealed by MEG. Nat Commun 7:11070.

Eggermont JJ (1991) Rate and synchronization measures of periodicity coding in cat primary auditory cortex. Hear Res 56:153–167.

Elias GA, Bieszczad KM, Weinberger NM (2015) Learning strategy refinement reverses early sensory cortical map expansion but not behavior: support for a theory of directed cortical substrates of learning and memory. Neurobiol Learn Mem 126:39–55.

Fitzpatrick DC, Roberts JM, Kuwada S, Kim DO, Filipovic B (2009) Processing temporal modulations in binaural and monaural auditory stimuli by neurons in the inferior colliculus and auditory cortex. J Assoc Res Otolaryngol 10:579–593.

Gervain J, Vines BW, Chen LM, Seo RJ, Hensch TK, Werker JF, Young AH (2013) Valproate reopens critical-period learning of absolute pitch. Front Syst Neurosci 7:102.

Goldberg JM, Brown PB (1969) Response of binaural neurons of dog superior olivary complex to dichotic tonal stimuli: some physiological mechanisms of sound localization. J Neurophysiol 32:613–636.

Gonzalez-Burgos G, Lewis DA (2008) GABA neurons and the mechanisms of network oscillations: implications for understanding cortical dysfunction in schizophrenia. Schizophr Bull 34:944–961.

Hitchcock LN, Raybuck JD, Wood MA, Lattal KM (2019) Effects of a histone deacetylase 3 inhibitor on extinction and reinstatement of cocaine self-administration in rats. Psychopharmacology (Berl) 236:517–529.

Hornickel J, Kraus N (2013) Unstable representation of sound: a biological marker of dyslexia. J Neurosci 33:3500–3504.

Hornickel J, Skoe E, Nicol T, Zecker S, Kraus N (2009) Subcortical differentiation of stop consonants relates to reading and speech-in-noise perception. Proc Natl Acad Sci U S A 106:13022–13027.

Hornickel J, Zecker SG, Bradlow AR, Kraus N (2012) Assistive listening devices drive neuroplasticity in children with dyslexia. Proc Natl Acad Sci U S A 109:16731–16736.

Joris PX, Schreiner CE, Rees A (2004) Neural processing of amplitude-modulated sounds. Physiol Rev 84:541–577.

Kato HK, Asinof SK, Isaacson JS (2017) Network-level control of frequency tuning in auditory cortex. Neuron 95:412–423.

Keeling MD, Calhoun BM, Krüger K, Polley DB, Schreiner CE (2008) Spectral integration plasticity in cat auditory cortex induced by perceptual training. Exp Brain Res 184:493–509.

Kraus N, Slater J, Thompson EC, Hornickel J, Strait DL, Nicol T, White-Schwoch T (2014) Music enrichment programs improve neural encoding of speech in at-risk children. J Neurosci 34:11913–11918.

Krizman J, Kraus N (2019) Analyzing the FFR: a tutorial for decoding the richness of auditory function. Hear Res 382:107779.

Krumbholz K, Patterson RD, Pressnitzer D (2000) The lower limit of pitch as determined by rate discrimination. J Acoust Soc Am 108:1170–1180.

Lakatos P, Karmos G, Mehta AD, Ulbert I, Schroeder CE (2008) Entrainment of neuronal oscillations as a mechanism of attentional selection. Science 320:110–113.

Leon MI, Poytress BS, Weinberger NM (2008) Avoidance learning facilitates temporal processing in the primary auditory cortex. Neurobiol Learn Mem 90:347–357.

Malvaez M, Sanchis-Segura C, Vo D, Lattal KM, Wood MA (2010) Modulation of chromatin modification facilitates extinction of cocaine-induced conditioned place preference. Biol Psychiatry 67:36–43.

Malvaez M, McQuown SC, Rogge GA, Astarabadi M, Jacques V, Carreiro S, Rusche JR, Wood MA (2013) HDAC3-selective inhibitor enhances extinction of cocaine seeking behavior in a persistent manner. Proc Natl Acad Sci U S A 110:2647–2652.

Mardia K (1972) Statistics of directional data. London: Academic.

McGaugh JL (2000) Memory—a century of consolidation. Science 287:248–251.

McQuown SC, Barrett RM, Matheos DP, Post RJ, Rogge GA, Alenghat T, Mullican SE, Jones S, Rusche JR, Lazar MA, Wood MA (2011) HDAC3 is a critical negative regulator of long-term memory formation. J Neurosci 31:764–774.

Miller LM, Escabí MA, Read HL, Schreiner CE (2002) Spectrotemporal receptive fields in the lemniscal auditory thalamus and cortex. J Neurophysiol 87:516–527.

Nakamura Y, Kimura S, Takada N, Takemura M, Iwamoto M, Hisaoka-Nakashima K, Nakata Y, Morioka N (2020) Stimulation of toll-like receptor 4 downregulates the expression of $\alpha 7$ nicotinic acetylcholine receptors via histone deacetylase in rodent microglia. Neurochem Int 138:104751.

Omote A, Jasmin K, Tierney A (2017) Successful non-native speech perception is linked to frequency following response phase consistency. Cortex 93:146–154.

Otto-Meyer S, Krizman J, White-Schwoch T, Kraus N (2018) Children with autism spectrum disorder have unstable responses to sound. Exp Brain Res 236:733–743.

Peelle JE, Gross J, Davis MH (2013) Phase-locked responses to speech in human auditory cortex are enhanced during comprehension. Cereb Cortex 23:1378–1387.

Phan ML, Bieszczad KM (2016) Sensory cortical plasticity participates in the epigenetic regulation of robust memory formation. Neural Plast 2016:7254297.

Phan ML, Gergues MM, Mahidadia S, Jimenez-Castillo J, Vicario DS, Bieszczad KM (2017) HDAC3 inhibitor RGFP966 modulates neuronal memory for vocal communication signals in a songbird model. Front Syst Neurosci 11:65.

Polley DB, Steinberg EE, Merzenich MM (2006) Perceptual learning directs auditory cortical map reorganization through top-down influences. J Neurosci 26:4970–4982.

Recanzone GH, Schreiner CE, Merzenich MM (1993) Plasticity in the frequency representation of primary auditory cortex following discrimination training in adult owl monkeys. J Neurosci 13:87–103.

Rotondo EK, Bieszczad KM (2020) Precise memory for pure tones is predicted by measures of learning-induced sensory system neurophysiological plasticity at cortical and subcortical levels. Learn Mem 27:328–339.

Rotondo EK, Bieszczad KM (2021) Sensory cortical and subcortical auditory neurophysiological changes predict cue-specific extinction enabled by the pharmacological inhibition of an epigenetic regulator during memory formation. Brain Res Bull 169:167–183.

Schroeder CE, Wilson DA, Radman T, Scharfman H, Lakatos P (2010) Dynamics of active sensing and perceptual selection. Curr Opin Neurobiol 20:172–176.

Selinger L, Zarnowiec K, Via M, Clemente IC, Escera C (2016) Involvement of the serotonin transporter gene in accurate subcortical speech encoding. J Neurosci 36:10782–10790.

Shang A, Bylipudi S, Bieszczad KM (2019) Inhibition of histone deacetylase 3 via RGFP966 facilitates cortical plasticity underlying unusually accurate auditory associative cue memory for excitatory and inhibitory cue-reward associations. Behav Brain Res 31:453–469.

Song JH, Skoe E, Wong PC, Kraus N (2008) Plasticity in the adult human auditory brainstem following short-term linguistic training. J Cogn Neurosci 20:1892–1902.

Stefanko DP, Barrett RM, Ly AR, Reolon GK, Wood MA (2009) Modulation of long-term memory for object recognition via HDAC inhibition. Proc Natl Acad Sci U S A 106:9447–9452.

Strait DL, Chan K, Ashley R, Kraus N (2012) Specialization among the specialized: auditory brainstem function is tuned in to timbre. Cortex 48:360–362.

Thompson EC, Woodruff Carr K, White-Schwoch T, Otto-Meyer S, Kraus N (2017) Individual differences in speech-in-noise perception parallel neural speech processing and attention in preschoolers. Hear Res 344:148–157.

Tierney AR, Krizman J, Kraus N (2015) Music training alters the course of adolescent auditory development. Proc Natl Acad Sci U S A 112:10062–10067.

Von Trapp G, Buran BN, Sen K, Semple MN, Sanes DH (2016) A decline in response variability improves neural signal detection during auditory task performance. J Neurosci 36:11097–11106.

White-Schwoch T, Nicol T, Warrier CM, Abrams DA, Kraus N (2017) Individual differences in human auditory processing: insights from single-trial auditory midbrain activity in an animal model. Cereb Cortex 27:5095–5115.

Yao JD, Sanes DH (2018) Developmental deprivation-induced perceptual and cortical processing deficits in awake-behaving animals. Elife:e33891.

Yao JD, Sanes DH (2021) Temporal encoding is required for categorization but not discrimination. Cereb Cortex 31:2886–2897.

Zhang J, Ma L, Li W, Yang P, Qin L (2016) Cholinergic modulation of auditory steady-state response in the auditory cortex of the freely moving rat. Neuroscience 324:29–39.

Zhou W, He Y, Rehman AU, Kong Y, Hong S, Ding G, Yalamanchili HK, Wan Y-W, Paul B, Wang C, Gong Y, Zhou W, Liu H, Dean J, Scalais E, O'Driscoll M, Morton JEV, Hou X, Wu Q, Tong Q, et al. (2019) Loss of function of NCOR1 and NCOR2 impairs memory through a novel GABAergic hypothalamus-CA3 projection. Nat Neurosci 22:205–217.